

1 **Reciprocal requirement of Wnt signaling and**  
2 **SKN-1 underlies cryptic intraspecies variation**  
3 **in an ancient embryonic gene regulatory**  
4 **network**

5

6

7

8 Yamila N. Torres Cleuren<sup>1,2\*</sup>, Chee Kiang Ewe<sup>2</sup>, Kyle C. Chipman<sup>2</sup>, Emily Mears<sup>1</sup>, Cricket G. Wood<sup>2</sup>,  
9 Coco A.E. Al-Alami<sup>1</sup>, Melissa R. Alcorn<sup>2</sup>, Thomas L. Turner<sup>3</sup>, Pradeep M. Joshi<sup>2</sup>, Russell G. Snell<sup>1</sup>, and  
10 Joel H. Rothman<sup>1,2,3</sup>

11

12 1. School of Biological Sciences, University of Auckland, Auckland, New Zealand

13 2. Department of MCD Biology and Neuroscience Research Institute, University of California Santa  
14 Barbara, CA, USA

15 3. Department of Ecology, Evolution, and Marine Biology, University of California Santa Barbara, CA,  
16 USA

17 \*Current address: Computational Biology Unit, Department of Informatics, University of Bergen,  
18 Bergen, 5020 Norway

19 Author for correspondence: [joel.rothman@lifesci.ucsb.edu](mailto:joel.rothman@lifesci.ucsb.edu)

20

21 **Keywords:** SKN-1, *C. elegans*, endoderm, GWAS, development, gene regulatory networks, Genotype-  
22 By-Sequencing, cryptic variation

23

24

25 **ABSTRACT**

26

27 Innovations in metazoan development arise from evolutionary modifications of gene  
28 regulatory networks (GRNs). We report large cryptic variation in the requirement for two key  
29 inputs, SKN-1/Nrf2 and MOM-2/Wnt, into the *C. elegans* endoderm-determining GRN. Some  
30 natural variants show a nearly absolute requirement for SKN-1 and MOM-2, while in others,  
31 most of the embryos differentiate endoderm in their absence. GWAS and analysis of  
32 recombinant inbred lines reveal multiple genetic regions underlying this broad phenotypic  
33 variation. A striking reciprocal relationship is seen in which genomic variants, or debilitation  
34 of genes involved in endoderm formation, that result in high SKN-1 requirement show low  
35 MOM-2/Wnt requirement and *vice-versa*. Thus, cryptic variation in the endoderm GRN may  
36 be tuned by opposing requirements for these two key regulatory inputs. These findings reveal  
37 that while the downstream components in the endoderm GRN are common across  
38 metazoans, initiating regulatory inputs are remarkable plastic even within a single species.

39

## 40 INTRODUCTION

41 While the core regulatory machinery that specifies embryonic germ layers and major  
42 organ identity in the ancestor of modern animals has been bequeathed to all extant animals,  
43 GRN architecture must be able to accommodate substantial plasticity to allow for  
44 evolutionary innovation in developmental strategies, changes in selective pressures, and  
45 genetic drift [1,2]. Genetic variation, often with neutral effects on fitness, provides for  
46 plasticity in GRN structure and implementation [2]. Although studies of laboratory strains of  
47 model organisms with a defined genetic background have been highly informative in  
48 identifying the key regulatory nodes in GRNs that specify developmental processes [3–5],  
49 these approaches do not reveal the evolutionary basis for plasticity in these networks. Which  
50 parameters of GRN architecture provide the greatest opportunity for genetically driven  
51 evolutionary change, and which are more rigidly fixed? The variation and incipient changes in  
52 GRN function and architecture can be discovered by analyzing phenotypic differences  
53 resulting from natural genetic variation present in distinct isolates of a single species [6–8].

54 The endoderm has been proposed to be the most ancient of the three embryonic  
55 germ layers in metazoans [9,10], having appeared prior to the advent of the bilateria about  
56 600 Mya [11]. It follows, therefore, that the GRN for endoderm in extant animals has  
57 undergone substantial modifications over the long evolutionary time span since its  
58 emergence. However, the core transcriptional machinery for endoderm specification and  
59 differentiation appears to share common mechanisms across metazoan phylogeny. For  
60 example, cascades of GATA-type transcription factors function to promote endoderm  
61 development not only in triploblastic animals but in the most ancient creatures that possess  
62 endoderm [12–16]. Among the many observations supporting a common regulatory

63 mechanism for establishing the endoderm, it has been found that the endoderm-determining  
64 GATA factor, END-1, in the nematode *C. elegans*, is sufficient to activate endoderm  
65 development in cells that would otherwise become ectoderm in *Xenopus* [17]. This indicates  
66 that the role of GATA factors in endoderm development has been preserved since the  
67 nematodes and vertebrates diverged from a common ancestor that lived perhaps 600 Mya.

68 To assess the genetic basis for evolutionary plasticity and cryptic variation underlying  
69 early embryonic germ layer specification, we have analyzed the well-described GRN for  
70 endoderm specification in *C. elegans*. The E cell, which is produced in the very early *C. elegans*  
71 embryo, is the progenitor of the entire endoderm, which subsequently gives rise exclusively  
72 to the intestine. The EMS blastomere at the four-cell stage divides to produce the E founder  
73 cell and its anterior sister, the MS founder cell, which is the progenitor for much of the  
74 mesoderm [18]. Both E and MS fates are determined by maternally provided SKN-1, an  
75 orthologue of the vertebrate Nrf2 bZIP transcription factor [19–21]. In the laboratory N2  
76 strain, elimination of maternal SKN-1 function (through either knock down or knockout)  
77 results in fully penetrant embryonic lethality as a result of misspecification of EMS cell  
78 descendants. In these embryos, the fate of MS is transformed to that of its cousin, the  
79 mesectodermal progenitor C cell. E cells similarly adopt a C cell-like fate in a majority, but not  
80 all, of these embryos [19]. SKN-1 initiates mesendoderm development via the GRN in E and  
81 MS cells in part by activating zygotic expression of the MED-1/2 divergent GATA transcription  
82 factors [22,23]. This event mobilizes a cascade of GATA factors in the E cell lineage that  
83 ultimately direct intestinal differentiation [21,24,25].

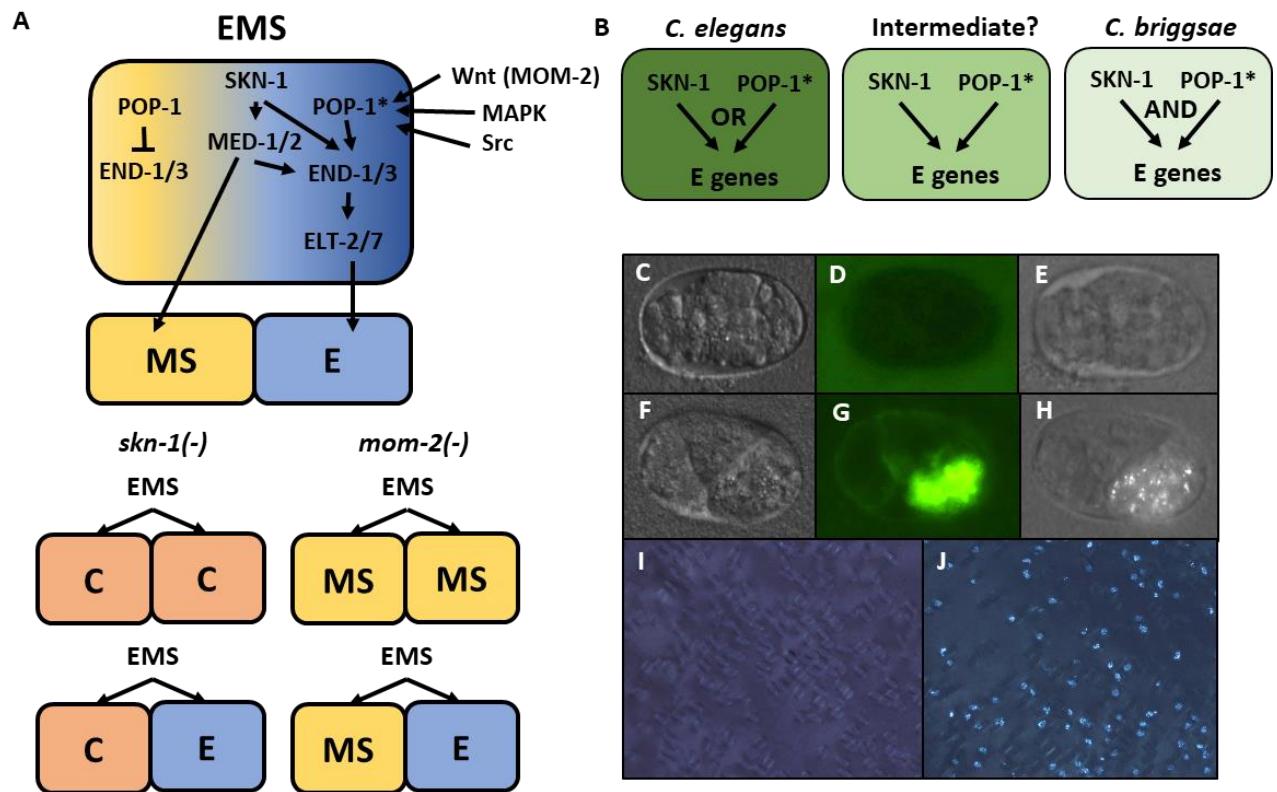
84 This differential requirement for SKN-1 in endoderm (E) and mesoderm (MS)  
85 development is determined by its combinatorial action with triply redundant Wnt, MAPK, and

86 Src signaling systems, which act together to polarize EMS [26–29]. MOM-2/Wnt acts through  
87 the MOM-5/Frizzled receptor, mobilizing WRM-1/ $\beta$ -catenin, resulting in its cytoplasmic  
88 accumulation in the posterior side of EMS. WRM-1, together with LIT-1/NLK kinase, alters  
89 both the nucleocytoplasmic distribution and activity of the Wnt effector POP-1/Tcf [29–31],  
90 converting it from a repressor of endoderm in the MS cell lineage to an activator in the E cell  
91 lineage [32–37]. Loss of MOM-2 expression in the laboratory N2 strain results in a partial  
92 gutless phenotype, while removal of both MOM-2 and SKN-1, through either knockdown or  
93 knockout, leads to a completely penetrant loss of gut [29], revealing their genetically  
94 redundant roles.

95         The regulatory relationship between SKN-1 and POP-1, the effector of Wnt signaling,  
96 shows striking variation even in relatively closely related species, suggesting substantial  
97 evolutionary plasticity in this key node in the endoderm GRN. *C. elegans* embryos lacking  
98 maternal POP-1 always make gut, both in the normal E cell lineage and in the MS cell lineage.  
99 However, in embryos lacking both SKN-1 and POP-1, endoderm is virtually never made,  
100 implying that these two factors constitute a Boolean “OR” logic gate. In contrast, removal of  
101 either SKN-1 or POP-1 alone in *C. briggsae* causes >90% of embryos to lack gut, indicative of  
102 an “AND” logic gate (Fig. 1A, B) [38].

103         In this study, we sought to determine whether the aforementioned changes in  
104 regulatory logic of the two major inputs into endoderm development are evident within the  
105 radiation of a single species. The availability of many naturally inbred variants (isotypes) of *C.*  
106 *elegans* that show widespread genomic variation [39–41], provides a genetically rich resource  
107 for investigating potential quantitative variation in developmental GRNs. We report here that  
108 the requirement for activation of the endoderm GRN by SKN-1 or MOM-2, but not POP-1, is

109 profoundly variable between natural *C. elegans* isolates, and even between very closely  
110 related isotypes. Thus, the key regulatory inputs into this major embryonic decision is subject  
111 to exceedingly rapid evolutionary modification. Genome-wide association studies in isolates  
112 from the natural populations and targeted analysis of recombinant inbred lines (RILs),  
113 revealed that a multiplicity of loci and their interactions are responsible for the variation in  
114 the developmental requirement for SKN-1 and MOM-2. We identified a striking reciprocal  
115 requirement for SKN-1 and MOM-2: loci associated with a high requirement for SKN-1 show  
116 a lower requirement for MOM-2 and *vice-versa*. We further identified several other  
117 endoderm regulatory factors, including RICT-1, PLP-1, and MIG-5, that show similar reciprocal  
118 relationships between these two GRN inputs. These findings reveal that the activation of the  
119 GRN network in specifying a germ layer, one of the most critical and early developmental  
120 switches in embryos, is subject to remarkable genetic plasticity during the radiation of a  
121 species and that the dynamic and rapid change in network architecture reflects influences  
122 distributed across many genetic components that affect both SKN-1 and Wnt pathways.



123  
124

125 **Fig 1. Endoderm regulatory pathway and scoring of gut differentiation.**

126 A) Under normal conditions, signaling from the posterior P<sub>2</sub> cell (Wnt, MAPK and Src) results in asymmetric  
 127 cortical localization of Wnt signaling pathway components in EMS leading to POP-1 asymmetry in the  
 128 descendants of EMS, with high levels of nuclear POP-1 in anterior MS and low levels of nuclear POP-1 in  
 129 the posterior, E, daughter cell. In the anterior MS cell, high nuclear POP-1 represses the END genes,  
 130 allowing SKN-1 to activate MS fate. In the posterior E cell, which remains in contact with P<sub>2</sub>, POP-1 is  
 131 converted to an activator and, along with SKN-1, activates the END genes, resulting in endoderm fate. Loss  
 132 of *skn-1*, either by RNAi or in loss-of-function mutants, causes 100% of the embryos to arrest; in 70% of the  
 133 arrested embryos, EMS gives rise to two C-like cells, while in the remaining 30% only MS is converted to a  
 134 C fate; the posterior daughter retains its E fate. Loss of *mom-2* leads to embryonic arrest with a partially  
 135 penetrant E→MS cell fate transformation, resulting in MS-like daughter cells. (B) Regulatory logic of SKN-1  
 136 and POP-1 in E specification in *C. elegans*, *C. briggsae* and a hypothetical intermediate state. POP-1\*  
 137 denotes the activated state. (C-H) Gut visualization in embryos affected by *skn-1* RNAi. (C-E) arrested  
 138 embryos without endoderm, (F-H) arrested embryos with endoderm. (C, F) DIC images of arrested embryos  
 139 ~12 hours after egg laying. (D, G) the same embryos expressing the gut-specific *elt-2::GFP* reporter, and  
 140 (E, H) birefringent gut granules under polarized light. All embryos showing gut birefringence also show  
 141 *elt-2::GFP* expression. (I, J) Fields of arrested *skn-1(RNAi)* embryos in wild isolate strains JU1491 (I) and JU440  
 142 (J), which reflect the extremes in the spectrum of requirement of SKN-1 in gut development at 0.9% and  
 143 60%, respectively.

## 144 MATERIALS AND METHODS

145

### 146 *C. elegans* strains and maintenance

147 All wild isolates, each with a unique haplotype [40], were obtained from the Caenorhabditis  
148 Genetics Center (CGC) (see Supplementary file 1). Worm strains were maintained as  
149 described [42] and all experiments were performed at 20°C unless noted otherwise. The  
150 following mutant and transgenic strains were used in this study: JJ185 *dpy-13(e184) skn-*  
151 *1(zu67) IV; mDp1 (IV;f)* , JR3666 (*elt-2::GFP X; (ifb-2::GFP) IV*, EU384 *dpy-11(e1180) mom-*  
152 *2(or42) V/nT1 [let-?(m435)] (IV;V)*, JJ1057 *pop-1(zu189) dpy-5(e61)/hT1 I; him-5(e1490)/hT1*  
153 *V*, KQ1366 (*rict-1(ft7) II*, SU351 *mig-5(rh94)/mIn1 [dpy-10(e128) mIs14] II*, and RB1711 *plp-*  
154 *1(ok2155) IV*.

### 155 RNAi

156 Feeding-based RNAi experiments were performed as described [43]. RNAi clones were  
157 obtained from either the Vidal [44] or Ahringer libraries [45]. RNAi bacterial strains were  
158 grown at 37°C in LB containing 50 µg/ml ampicillin. The overnight culture was then diluted  
159 1:10. After 4 hours of incubation at 37°C, 1 mM of IPTG was added and 60µl was seeded onto  
160 35mm agar plates containing 1 mM IPTG and 25 µg/ml carbenicillin. Seeded plates were  
161 allowed to dry and used within five days. Five to 10 L4 animals were placed on RNAi plate. 24  
162 hours later, they were transferred to another RNAi plate and allowed to lay eggs for four or  
163 12 hours (12 hours for *skn-1* RNAi and four hours for the other RNAi). The adults were then  
164 removed, leaving the embryos to develop for an extra 7-9 hours. Embryos were quantified  
165 and imaged on agar pad using Nikon Ti-E inverted microscope.

### 166 Antibody staining



167 The embryonic gut cells and nuclei of all cells were stained with MH33 (mouse anti-IFB-2,  
168 deposited to the DSHB by Waterston, R.H.) and AHP418 (rabbit anti-acetylated histone H4,  
169 Serotec Bio-Rad) respectively. Fixation and permeabilization were carried out as described  
170 previously [46]. Goat anti-mouse Alexa Fluor® 594 and goat anti-rabbit Alexa Fluor® 488  
171 secondary antibodies were used at 1:1000 dilution.

## 172 **Quantification of endoderm specification**

173 Gut was scored by presence of birefringent gut granule in arrested embryos [47,48]. For *skn-*  
174 *1(RNAi)*, the laboratory strain N2, which shows invariable ~30% of embryos with endoderm,  
175 was used as a control for all experiments.

## 176 **Introgression of *skn-1(zu67)*, *pop-1(zu189)*, and *mom-2(or42)* alleles into wild isolate** 177 **backgrounds**

178 To introgress *skn-1(zu67)* into wild isolates (WI), males from the wild isolate strains were  
179 crossed to JJ186 *dpy-13(e184) skn-1(zu67) IV; mDp1 (IV;f)* hermaphrodites. *mDp1* is a free  
180 duplication that rescues the Dpy and lethal phenotypes of *dpy-13(e184)* and *skn-1(zu67)*  
181 respectively. Animals that have lost the free duplication will be Dpy and produce dead  
182 offspring. Wild type F1 hermaphrodites that have lost the free duplication as determined by  
183 presence of a ¼ Dpy progeny in the F2 were selected. 10 single non-Dpy F2 hermaphrodite  
184 descendants from F1 animals heterozygous for *skn-1(zu67)* (2/3 of which would be of the  
185 genotype *WI dpy-13(+) skn-1(+)/ dpy-13(e184) skn-1(zu67)* were backcrossed to their  
186 respective parental wild strain. 10 F3 hermaphrodites were picked to individual plates. Half  
187 of the F3 cross progeny would be heterozygous for *dpy-13(e184) skn-1(zu67)*, as evidenced  
188 by presence of F4 Dpy progeny that produced dead embryos. Non-Dpy siblings were used to  
189 continue the introgression as described. This was repeated for at least 5 rounds of

190 introgression. The embryonic gutless phenotype in the progeny of the Dpy animals was  
191 quantified.

192 Similarly, to introgress *pop-1(zu189)* or *mom-2(or42)* alleles into wild isolates, JJ1057  
193 *pop-1(zu189) dpy-5(e61)/hT1 I*; *him-5(e1490)/hT1V* or EU384 *dpy-11(e1180) mom-2(or42)*  
194 *V/nT1 [let-?(m435)] (IV;V)* were used, respectively. The mutant strain was crossed to the wild  
195 isolates. Non-Dpy F2 animals heterozygous for the chromosomal mutation were selected and  
196 backcrossed to their respective parental wild strain for at least four rounds of introgression  
197 for *pop-1* and seven rounds for *mom-2*. The embryonic gutless phenotype in the progeny of  
198 the Dpy animals was quantified, as above.

#### 199 **Statistical Analyses: GWAS and EMMA**

200 All data were analyzed and plotted using R software v 3.2.3 ([https://www.r-](https://www.r-project.org/)  
201 [project.org/](https://www.r-project.org/)). GWAS for both phenotypes was performed using *C. elegans* wild isolates and  
202 a previously published SNP map containing 4,690 SNPs [40] with the EMMA R package. P-  
203 values were calculated using mixed model analysis [49] (`emma.REML.t()` function) and IBS  
204 kinship matrix to account for population structure. For *skn-1* and *mom-2* RNAi phenotypic  
205 data, a genome-wide permutation-based FDR was also calculated for the EMMA results from  
206 10,000 permuted values [50,51]. In addition, a linear model GWAS was performed with the  
207 same SNP map (but no kinship matrix) on both *mom-2* and *skn-1* datasets, with FDR  
208 calculations obtained from 10,000 permuted values. However, owing to the skewed nature  
209 of the *mom-2(RNAi)* data (Supplementary Fig. 4), genome-wide permutation-based FDR  
210 thresholds did not reveal any significant loci. The p-values for each individual SNP were then  
211 adjusted based on 1000 permutations at each locus. Significance thresholds were set at  
212  $p < 0.01$  and  $0.001$ .

## 213 **Phylogenetic and geographical analyses**

214 Phylogenetic trees were constructed from 4,690 polymorphisms using R package  
215 "ape". Neighbor-joining algorithm based on pairwise distances was used. Correlations  
216 between phenotypes and phylogeny were calculated using a Mantel test. Bayesian  
217 interference was used to estimate phylogenetic relatedness amongst the isotypes.  
218 Phenotypic similarity was quantified using Euclidean distance across both SKN-1 and MOM-2  
219 phenotypes.

220 Geographic information for strains were obtained from Andersen *et al.* [40], available in  
221 Supplementary Files 5 and 6, together with the corresponding phenotypes.

## 222 **Correlation Analysis**

223 In order to test for the relationship between *mom-2 (RNAi)* and *skn-1 (RNAi)* phenotypic data,  
224 the difference between median phenotypic values for each SNP were calculated  
225 independently on both a genome-wide level (N = 4690) and at the SNPs most significantly  
226 associated with the *mom-2 (RNAi)* phenotype (N = 45,  $p < 0.01$ ). Pearson's correlation test  
227 was used to calculate correlation between median phenotypic values for genome-wide  
228 analysis using a sliding window (N = 50 SNPs). Spearman's Rho was used to calculate the  
229 correlation using only SNPs most significantly associated with *mom-2* GWAS.

## 230 **RIL construction and Genotype-By-Sequencing (GBS)**

231 Recombinant inbred lines (RILs) were created by crossing an N2 hermaphrodite and an MY16  
232 male. 120 F2 progeny were cloned to individual plates and allowed to self-fertilize for 10  
233 generations. A single worm was isolated from each generation to create inbred lines. A total

234 of 95 lines were successfully created and frozen stocks were immediately created and kept at  
235 -80°C (Supplementary Files 3 and 4), prior to DNA sequencing.

236 DNA was extracted using Blood and Tissue QIAGEN kit from worms from each of the RILs  
237 grown on four large NGM plates (90x15mm) with OP50 *E. coli* until starved (no more than a  
238 day). Samples were submitted in 96-well plate format at 10 ng/μl < n < 30 ng/μl. GBS libraries  
239 were constructed using digest products from ApeKI (GWCGC), using a protocol modified from  
240 [52]. After digestion, the barcoded adapters were ligated and fragments < 100bp were  
241 sequenced as single-end reads using an Illumina HiSeq 2000 lane (100 bp, single-end reads).

242 SNP calling was performed using the GBSversion3 pipeline in Trait Analysis by aSSociation,  
243 Evolution and Linkage (TASSEL) [53]. Briefly, fastq files were aligned to reference genome  
244 WS252 using BWA v. 0.7.8-r455 and SNPs were filtered using vcftools [54]. Samples with  
245 greater than 90% missing data and SNPs with minor allele frequencies (MAF) of <1% were  
246 excluded from analysis, identifying 27,396 variants.

#### 247 **QTL mapping using R/qtl**

248 Variants identified by GBS pipeline were filtered to match the SNPs present in the parental  
249 MY16 strain (using vcftools --recode command), and variants were converted to a 012 file  
250 (vcftools --012 command). Single-QTL analysis was performed in R/QTL [55] using 1770  
251 variants and 95 RILs. Significant QTL were determined using Standard Interval Mapping  
252 (scanone() "em") and genome-wide significance thresholds were calculated by permuting the  
253 phenotype (N =1,000). Change in log-likelihood ratio score of 1.5 was used to calculate 95%  
254 confidence intervals and define QTL regions [56]. Genetic maps and the corresponding  
255 phenotypes used in analysis available in Supplementary Files 3 and 4.

256 **RESULTS**

257 **Extensive natural cryptic variation in the requirement for SKN-1 in endoderm specification**  
258 **within the *C. elegans* species**

259           The relationship between SKN-1 and Wnt signaling through POP-1 in the endoderm  
260 GRN has undergone substantial divergence in the *Caenorhabditis* genus [38]. While neither  
261 input alone is absolutely required for endoderm specification in *C. elegans*, each is essential  
262 in *C. briggsae*, which has been estimated to have diverged from *C. elegans* ~20-40 Mya  
263 [57,58]. In contrast to the *C. elegans* N2 laboratory strain, removal of either SKN-1 or POP-1  
264 alone results in fully penetrant conversion of the E founder cell fate into that of the  
265 mesectodermal C blastomere and of E to MS fate, respectively, in *C. briggsae* [38]. These  
266 findings revealed that the earliest inputs into the endoderm GRN are subject to substantial  
267 evolutionary differences between these two species (Fig. 1B). We sought to determine  
268 whether incipient evolutionary plasticity in this critical node at the earliest stages of  
269 endoderm development might be evident even within a single species of the *Caenorhabditis*  
270 genus by assessing their requirement in *C. elegans* wild isolates and testing whether the  
271 quantitative requirements of each input were correlated.

272           Elimination of detectable maternal SKN-1 from the laboratory N2 strain by either a  
273 strong (early nonsense) chromosomal mutation (*skn-1(zu67)*), or by RNAi knockdown, results  
274 in a partially penetrant phenotype: while the E cell adopts the fate of the C cell in the majority  
275 of embryos, and gut is not made, ~30% of arrested embryos undergo strong gut  
276 differentiation, as evidenced by the appearance of birefringent, gut-specific rhabditin  
277 granules, or expression of *elt-2::GFP*, a marker of the developing and differentiated intestine  
278 (Fig. 1C-H). We found that RNAi of *skn-1* in different N2-derived mutant strains gave highly

279 reproducible results: 100% of the embryos derived from *skn-1(RNAi)*-treated mothers arrest  
280 ( $n > 100,000$ ) and  $32.0 \pm 1.9\%$  of the arrested embryos exhibited birefringent gut granules (Fig.  
281 2A; Supplementary Fig. 1). We found that the LSJ1 laboratory strain, which is derived from  
282 the same original source as N2, but experienced very different selective pressures in the  
283 laboratory owing to its constant propagation in liquid culture over 40 years [59], gave virtually  
284 identical results to that of N2 ( $31.0\% \pm \text{s.d. } 1.2\%$ ), implying that SKN-1-independent endoderm  
285 formation is a quantitatively stable trait. The low variability in this assay, and high number of  
286 embryos that can be readily examined ( $\geq 500$  embryos per experiment), provides a sensitive  
287 and highly reliable system with which to analyze genetic variation in the endoderm GRN  
288 between independent *C. elegans* isolates.

289 To assess variation in SKN-1 requirement within the *C. elegans* species, we analyzed  
290 the outcome of knocking down SKN-1 by RNAi in 96 unique *C. elegans* wild isolates [40].  
291 Owing to their propagation by self-fertilization, each of the isolates (isotypes) is a naturally  
292 inbred clonal population that is virtually homozygous and defines a unique haplotype. The  
293 reported estimated population mutation rate averages  $8.3 \times 10^{-4}$  per bp [40], and we found  
294 that a substantial fraction (29/97) of isotypes were quantitatively indistinguishable in  
295 phenotype between the N2 and LSJ1 laboratory strains (Fig. 2A, Supplementary File 1). We  
296 found that all strains, with the exception of the RNAi-resistant Hawaiian CB4856 strain,  
297 invariably gave 100% embryonic lethality *with skn-1(RNAi)*, showing that on the basis of that  
298 criterion all strains are fully sensitive to RNAi. However, we observed dramatic variation in  
299 the fraction of embryos with differentiated gut across the complete set of strains, ranging  
300 from 0.9% to 60% (Fig. 2A). Repeated measurements with  $> 500$  embryos per replicate per  
301 strain revealed very high reproducibility (Supplementary Fig. 1), indicating that even small  
302 differences in the fraction of embryos generating endoderm could be reproducibly measured.

303 Further, we found that some wild isolates that were subsequently found to have identical  
304 genome sequences also gave identical results. We note that these results contrast with those  
305 of Paaby *et al.* [60], who found that RNAi in liquid culture of a set of 55 wild isolates resulted  
306 in much weaker effects, both on lethality and on gut differentiation. This difference is likely  
307 attributable to variability in RNAi efficacy in the latter study [61,62].

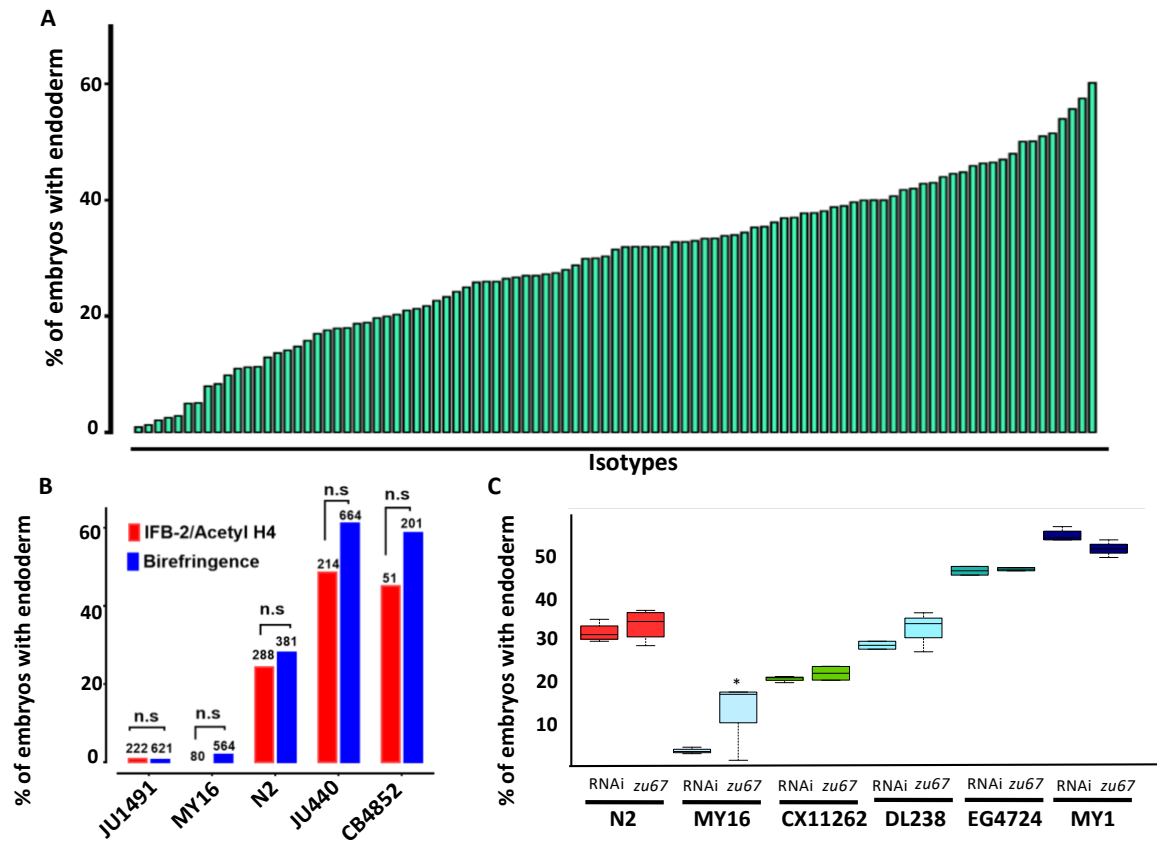
308         Although birefringent and autofluorescent rhabditin granules have been used as a  
309 marker of gut specification and differentiation in many studies [47,48], it is conceivable that  
310 the variation in fraction of embryos containing this marker that we observed might reflect  
311 variations in gut granule formation rather than in gut differentiation *per se*. We note that  
312 embryos from all strains showed a decisive “all-or-none” phenotype: i.e., they were either  
313 strongly positive for gut differentiation or completely lacked gut granules, with virtually no  
314 intermediate or ambiguous phenotypes. A threshold of gene activity in the GRN has been  
315 shown to account for such an all-or-none switch in gut specification [22,63,64]. This  
316 observation is inconsistent with possible variation in gut granule production: if SKN-1-  
317 depleted embryos were defective in formation of the many granules present in each gut cell,  
318 one might expect to observe gradations in numbers or signal intensity of these granules  
319 between gut cells or across a set of embryos. Nonetheless, we extended our findings by  
320 analyzing expression of the gut-specific intermediate filament IFB-2, a marker of late gut  
321 differentiation, in selected strains representing the spectrum of phenotypes observed (Fig.  
322 2B). As with gut granules, we found that embryos showed all-or-none expression of IFB-2. In  
323 all cases, we found that the fraction of embryos containing immunoreactive IFB-2 was not  
324 significantly different (Fisher’s exact test, p-values > 0.05) from the fraction containing gut  
325 granules, strongly suggesting that the strains vary in endoderm specification *per se* and  
326 consistent with earlier studies of SKN-1 function [19,22].

327           Although we found that *skn-1(RNAi)* was 100% effective at inducing embryonic  
328 lethality in all strains (with the exception of the RNAi-defective Hawaiian strain, CB4856), it is  
329 conceivable that, at least for the strains that showed a weaker phenotype than for N2 (i.e.,  
330 higher number of embryos specifying endoderm), the variation observed between strains  
331 might be attributable to differences in RNAi efficacy rather than in the endoderm GRN. To  
332 address this possibility, we introgressed the strong loss-of-function *skn-1(zu67)* chromosomal  
333 mutation into five wild isolates whose phenotypes spanned the spectrum observed (ranging  
334 from 2% of embryos with differentiated gut for MY16 to 50% for MY1) (Fig. 2C). In all cases,  
335 we found that introgression of the allele through five rounds of backcrosses resulted in a  
336 quantitative phenotype that was similar or identical to that of the effect observed with *skn-*  
337 *1(RNAi)*. The phenotypes of the introgressed allele were significantly different (p-values  
338 <0.01) from that of the parental N2 *skn-1(zu67)* strain, except for DL238, whose *skn-1(RNAi)*  
339 phenotype was indistinguishable from that of N2. The results obtained by introgression from  
340 four of the isotypes (CX11262, DL238, EG4724 and MY1), were not statistically different  
341 (Student t-test, p-values >0.05) from the corresponding RNAi knock down results (Fig. 2C)  
342 (i.e., the phenotype was suppressed or enhanced relative to N2 in these genetic backgrounds  
343 to the same extent as with *skn-1(RNAi)*). However, while the MY16 *skn-1(zu67)* strain shifted  
344 in the predicted direction (i.e., became stronger) when compared to the N2 strain, it was a  
345 weaker effect than was evident by RNAi knockdown, even following eight rounds of  
346 introgression. Nonetheless, diminished RNAi efficacy in MY16 cannot explain the large  
347 difference in *skn-1(RNAi)* phenotype between N2 and MY16, as the latter phenotype is much  
348 stronger, not weaker, than the former. As described below, we identified a modifier locus in  
349 the MY16 strain that is closely linked to the *skn-1* gene; it seems likely that the N2  
350 chromosomal segment containing this modifier was carried with the *skn-1(zu67)* mutation



351 through the introgression crosses, thereby explaining the somewhat weaker phenotype of  
352 the introgressed allele compared to the RNAi effect in MY16. The results of introgression of  
353 the *skn-1(zu67)* chromosomal mutation confirm that the extreme variation in *skn-1(RNAi)*  
354 phenotype between the wild isolates results from *bona fide* cryptic variation in the endoderm  
355 GRN, rather than differences in RNAi efficacy.

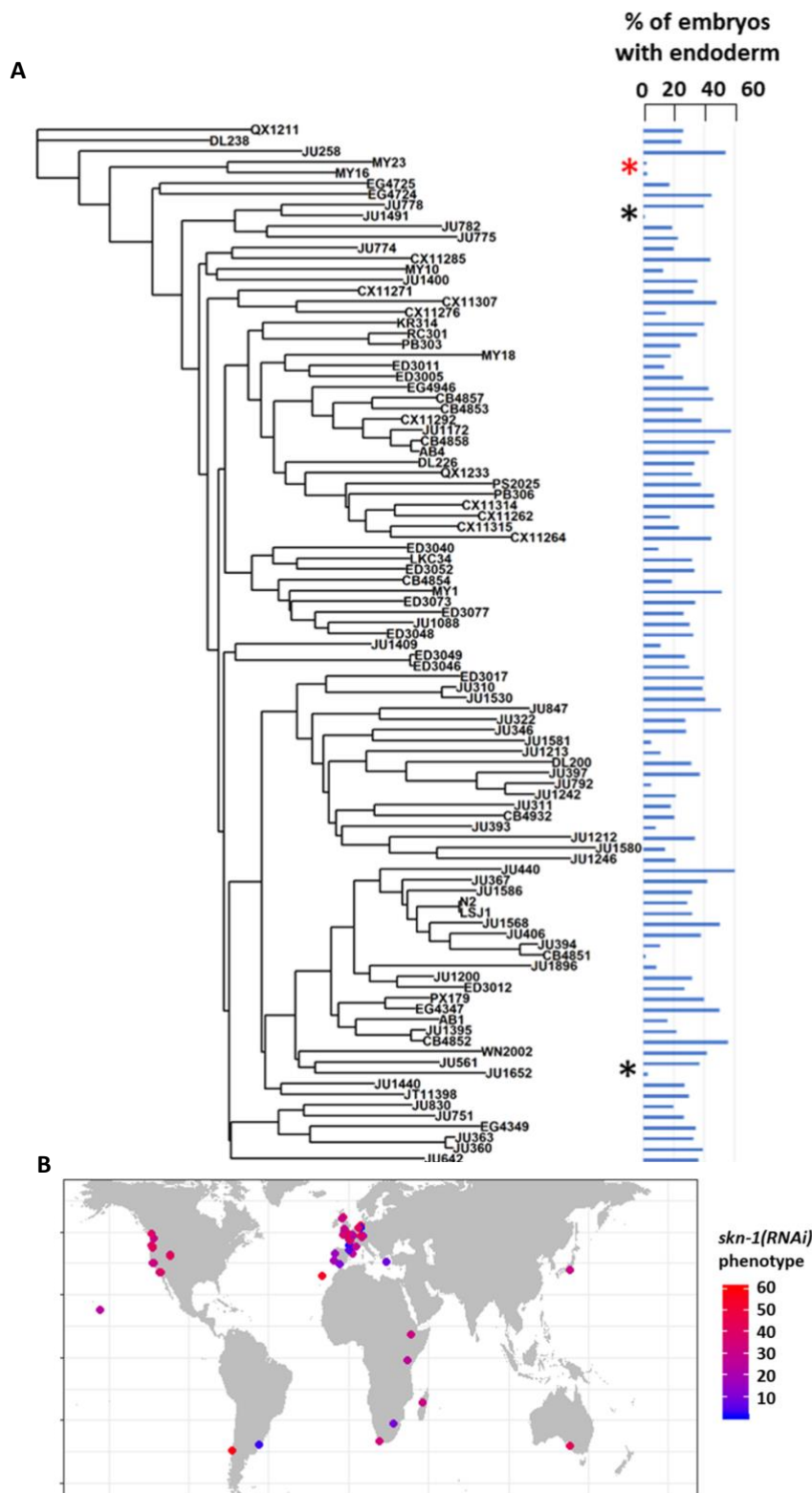
356 We note that the strength of *skn-1(RNAi)* phenotype does not correlate with  
357 phylogenetic relatedness between the strains (Mantel test  $r = 0.21$ , NS). To illustrate, while  
358 some closely related strains (e.g., MY16 and MY23) showed a similar gut developmental  
359 phenotype, some very closely related strains (e.g., JU1491 and JU778) had phenotypes on the  
360 opposite ends of the phenotypic spectrum (Fig. 3A). We also did not observe any clear  
361 association between geographical distribution and *skn-1 (RNAi)* phenotype (Fig. 3B). These  
362 findings suggest that the endoderm GRN may be subject to rapid intraspecies evolutionary  
363 divergence and suggests that a small number of loci may underlie variation in the trait.



364

365 **Fig. 2: Quantitative effects of loss of *skn-1* on endoderm formation.**

366 (A) Spectrum of *skn-1(RNAi)* effects across the *C. elegans* isolates. The effects of *skn-1(RNAi)* are quantified  
 367 as the average percentage of arrested embryos with endoderm (y-axis). All wild isolates treated with *skn-1(RNAi)*  
 368 resulted in 100% embryonic arrest ( $n > 500$  embryos per replicate per isotype and at least two  
 369 replicates per isotype). (B) Comparison of *skn-1(RNAi)* phenotype using two different gut markers  
 370 (birefringent gut granules and MH33 staining of IFB-2) in five different genetic backgrounds. In all cases,  
 371 no significant statistical difference was found between the two quantitative methods. Fisher's exact test  
 372 (NS  $p$ -value  $> 0.05$ ). (C) Comparison of *skn-1(RNAi)* and *skn-1(zu67)* effects on endoderm development in six  
 373 different genetic backgrounds. For each color-coded strain, the first value is of the *skn-1(RNAi)* results (five  
 374 replicates), while the second is the result for the *skn-1(zu67)* allele introgression (10 replicates). For all  
 375 strains (with the exception of MY16), no significant statistical difference was found between the RNAi  
 376 knockdown and corresponding *skn-1(zu67)* allele effects on endoderm development. Student t-test (NS  $p$ -  
 377 value  $> 0.05$ , \*  $p$ -value  $< 0.05$ ).



378  
 379 **Fig. 3: SKN-1 requirement does not correlate with genotypic relatedness or geographical location.**  
 380 (A) *skn-1(RNAi)* phenotype of 97 isolates arranged with respect to the neighbor-joining tree constructed  
 381 using 4,690 SNPs and pseudo-rooted to QX1211. Red asterisk indicates an example of closely related strains  
 382 (MY23 and MY16) with similar phenotype, while black asterisks indicate example sister strains (JU778 and  
 383 JU1491; JU561 and JU1652) with distinct phenotype. Phylogenetic relatedness and phenotype (measured  
 384 as Euclidean distance) are not significantly correlated (Mantel test,  $r = 0.21$ , NS). (B) Worldwide distribution  
 385 of *skn-1(RNAi)* phenotype across 97 wild isolates. Each circle represents a single isotype.

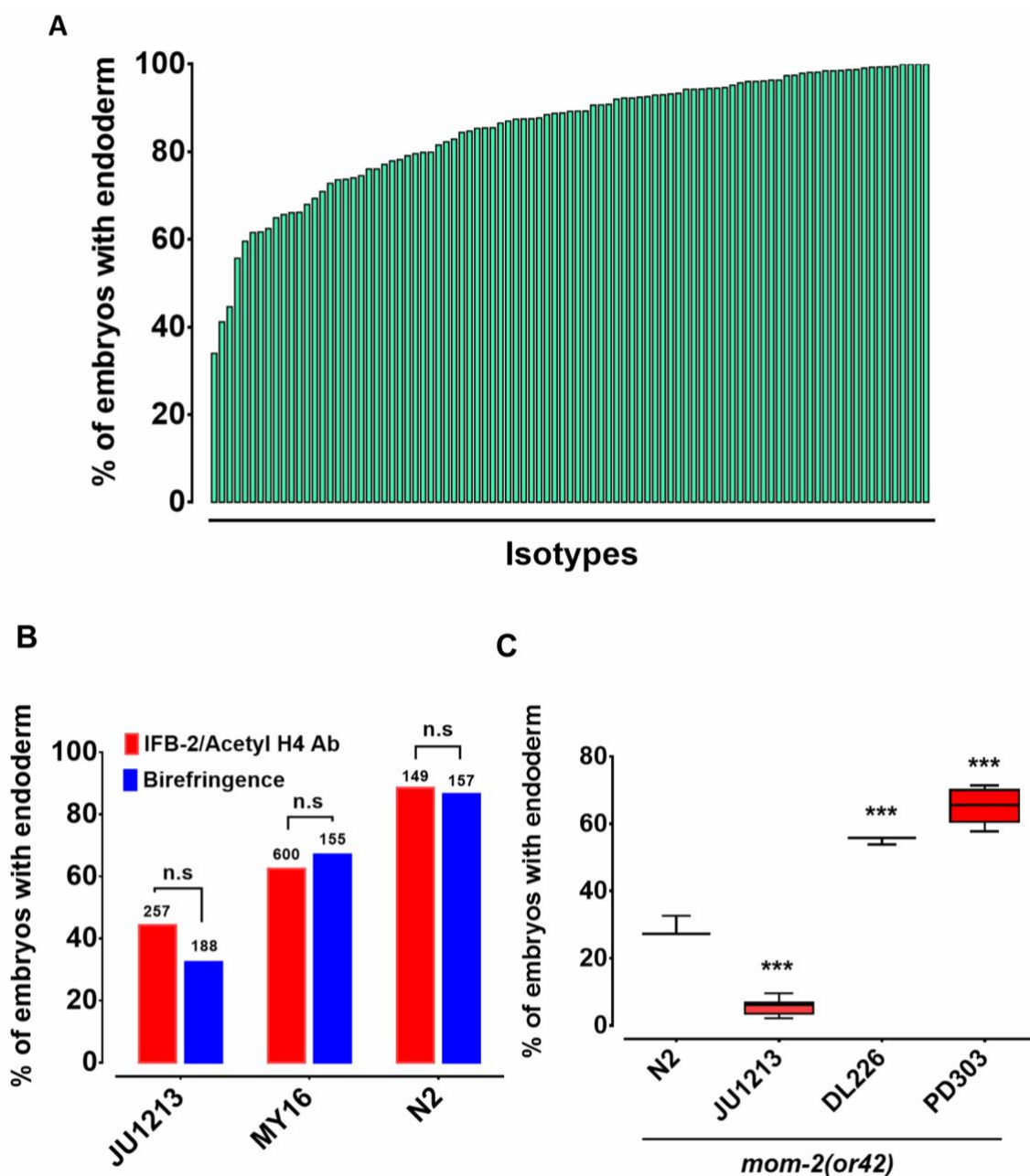
386 **Cryptic variation in the quantitative requirement for MOM-2 Wnt, but not POP-1, in**  
387 **endoderm development**

388 The switch in the relationship of the SKN-1 and Wnt inputs between *C. elegans* (“OR”  
389 operator) and *C. briggsae* (“AND” operator) [38], and the extensive variation in the  
390 requirement for SKN-1 seen across *C. elegans* isolates, raised the possibility that the  
391 quantitative requirement for Wnt components might vary between unique isolates of *C.*  
392 *elegans*. It has been shown that signaling from Ras pathway varies in different *C. elegans* wild  
393 isolates and hyperactive Wnt signaling can compensate for reduced Ras activity in the vulva  
394 signaling network [6,65]. Given that removal of the maternal Wnt input also results in a  
395 partially penetrant gut defect (through either knock-out or knockdown of Wnt signaling  
396 components), it is conceivable that a compensatory relationship may exist between the SKN-  
397 1 and Wnt inputs. We investigated this possibility by examining the requirement for the  
398 MOM-2/Wnt ligand in the same wild isolates that were tested for the SKN-1 gut  
399 developmental requirement. Indeed, we observed broad variation in the requirement for  
400 MOM-2/Wnt in activation of the endoderm GRN between isotypes. *mom-2(RNAi)* of 94  
401 isotypes resulted in embryonic arrest, indicating that, as with *skn-1(RNAi)*, *mom-2(RNAi)* was  
402 effective at least by the criterion of lethality. Two isotypes, CB4853 and EG4349, did not  
403 exhibit *mom-2(RNAi)*-induced lethality and were omitted from further analyses. In the  
404 affected strains, the fraction of *mom-2(RNAi)* embryos with differentiated gut varied from  
405 ~40% to ~99% (Fig. 4A, Supplementary File 2). As with *skn-1(RNAi)*, the *mom-2(RNAi)*  
406 phenotype of isotypes N2, JU440, and JU1213 was further confirmed by immunostaining with  
407 IFB-2 (Fig 4B), again demonstrating that birefringence of gut granules is a reliable proxy for  
408 endoderm formation for this analysis.

409 To assess whether the observed variation in the *mom-2(RNAi)* phenotype reflected  
410 differences in the GRN or RNAi efficacy, the *mom-2(or42)* allele was introgressed into three  
411 different genetic backgrounds chosen from the extreme ends of the phenotypic spectrum.  
412 *mom-2(RNAi)* of the laboratory N2 strain resulted in the developmental arrest of embryos. Of  
413 those, ~90% contained differentiated endoderm, a result that was highly reproducible. In  
414 contrast, the introgression of an apparent loss-of-function allele, *mom-2(or42)*, into the N2  
415 strain results in a more extreme phenotype: only ~28% of embryos show endoderm  
416 differentiation (Fig. 4C) [29]. While this discrepancy can partly be explained by incomplete  
417 RNAi efficacy, it is notable that the penetrance of *mom-2* alleles vary widely [29]. We  
418 observed strain-specific variation in embryonic lethality response to RNAi of *mom-2* between  
419 the different isotypes. However, we found that the *mom-2(or42)* introgressed strains show  
420 qualitatively similar effects to those observed with *mom-2* RNAi. For example, the *mom-*  
421 *2(or42)* allele introgressed into the isotype JU1213 background resulted in a severe gutless  
422 phenotype ( $5.7\% \pm \text{s.d } 2.4\%$ ;  $n=2292$ ) a similar but more extreme effect than was seen with  
423 RNAi ( $34.0\% \pm \text{s.d } 1.5\%$ ;  $n=1876$ ). This is the strongest phenotype that has been reported for  
424 any known *mom-2* allele. On the other hand, introgression of the *mom-2* mutation gave rise  
425 to a significantly higher fraction of embryos with endoderm in isotypes DL226 ( $55.2\% \pm \text{s.d}$   
426  $1.2\%$ ,  $n=1377$ ) and PB303 ( $65.5\% \pm \text{s.d } 4.9\%$ ,  $n=2726$ ), relative to the laboratory strain N2  
427 ( $29.1\% \pm \text{s.d } 3.1\%$ ;  $n=1693$ ), consistent with the RNAi phenotypes (Fig. 4C). These findings  
428 indicate that the differential requirement for MOM-2 is, at least in part, attributable to  
429 genetic modifiers in these strains.

430 As the MOM-2/Wnt signal is mediated through the POP-1 transcription factor, we  
431 sought to determine whether the requirement for POP-1 might also vary between isolates.  
432 We found that, while *pop-1(RNAi)* resulted in 100% embryonic lethality across all 96 RNAi-

433 sensitive isolates, 100% of the arrested embryos contained a differentiated gut (n>500 for  
434 each isolate scored) (results not shown). Thus, all isolates behave similarly to the N2 strain  
435 with respect to the requirement for POP-1. These results were confirmed by introgressing a  
436 strong loss-of-function *pop-1(zu189)* allele into four wild isolates (N2, MY16, JU440, and  
437 KR314) (Supplementary Fig. 2). The lack of variation in endoderm specification after loss of  
438 POP-1 is not entirely unexpected. As has been observed in a *pop-1(-)* mutant strain,  
439 elimination of the endoderm-repressive role of POP-1 in the MS lineage (which is not  
440 influenced by the P2 signal) supersedes its endoderm activating role in the presence of SKN-  
441 1. Indeed, the original observation that all *pop-1(-)* embryos in an N2 background contain gut  
442 masked the activating function for POP-1, which is apparently only in the absence of SKN-1  
443 [32,34,36]. It is likely that, as with the N2 strain, gut arises from both E and MS cells in all of  
444 these strains; however, as we have scored only for presence or absence of gut, it is  
445 conceivable that the E lineage is not properly specified in some strains, a possibility that  
446 cannot be ruled out without higher resolution analysis.



447

448 **Fig. 4: Widespread variation in the *mom-2(RNAi)* phenotype.**

449 (A) Spectrum of *mom-2(RNAi)* effects across the *C. elegans* isolates. The effects of *mom-2(RNAi)* are  
 450 quantified as the average percentage of arrested embryos with endoderm (y-axis). Each column represents  
 451 the mean for each wild isolate (n >500 embryos were scored for each experiment with at least two  
 452 replicates per isotype). (B) Comparison of *mom-2(RNAi)* phenotype using two different gut markers  
 453 (birefringent gut granules and MH33 staining of IFB-2) in three different genetic backgrounds. In all cases,  
 454 no significant statistical difference was found between the two quantitative methods. Fisher's exact test  
 455 (NS p-value>0.05). (C) Comparison of the effect of *mom-2(or42)* on endoderm development after  
 456 introgression into four different genetic backgrounds. At least three independent introgressed lines were  
 457 studied for each wild isotype. The results were compared to *N2; mom-2(or42)*. Student t-test (\*\*\*) p-  
 458 value<0.001).

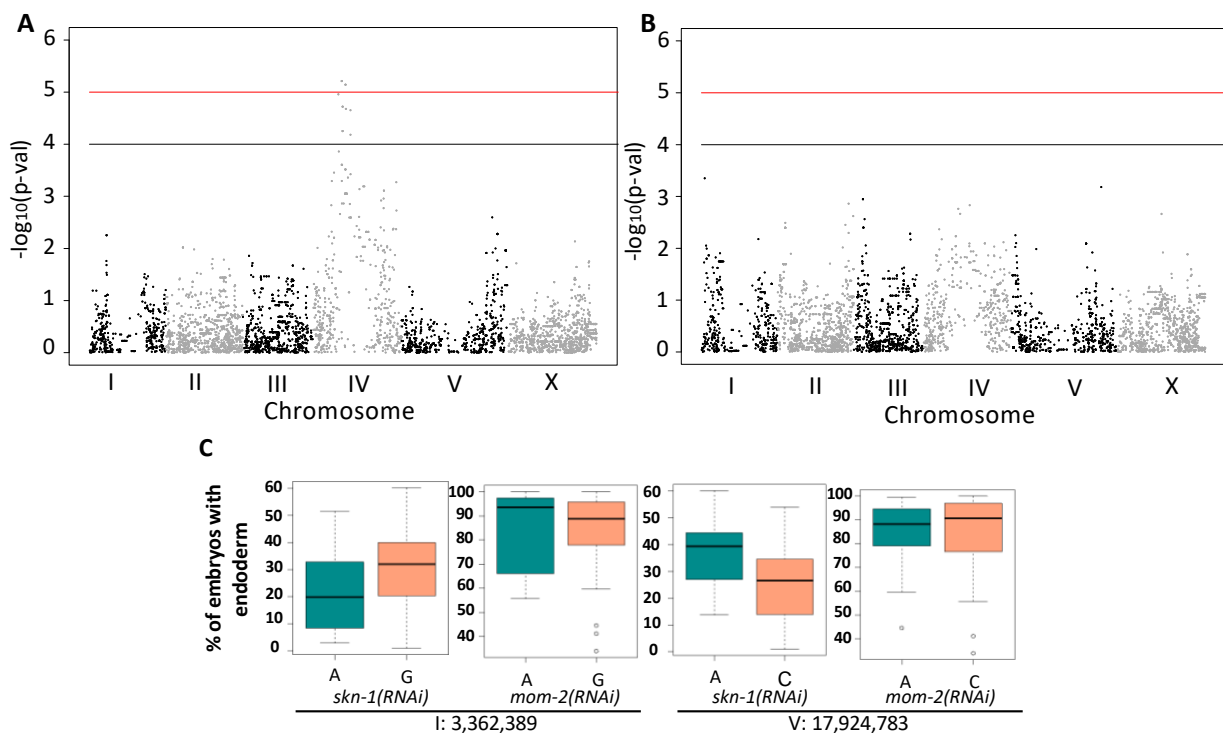
459 **Genome-wide association studies (GWAS) and analysis of RILs identify multiple genomic**  
460 **regions underlying variation in the two major endoderm GRN inputs**

461 We sought to examine the genetic basis for the wide variation in SKN-1 and Wnt  
462 requirements across *C. elegans* isolates and to evaluate possible relationships in the variation  
463 seen with the SKN-1 and Wnt inputs by performing linear-model GWAS using the available  
464 SNP markers and map [40]. This analysis identified two highly significantly associated regions  
465 on chromosomes IV and V (FDR < 1.5) that underlie the variation in SKN-1 requirement  
466 (Supplementary Fig. 3A). To ensure that these two QTLs were not an artifact of genetic  
467 relatedness between sets of strains, we applied the more stringent EMMA (Efficient Mixed-  
468 Model Analysis) algorithm, which adjusts for population structure (Fig. 5A) [49,66]. This  
469 approach also identified the same significant location on chromosome IV. The two mapping  
470 approaches show a moderate linear correlation (Spearman correlation coefficient = 0.43)  
471 (Supplementary Fig. 3B). In each case, the most statistically significant SNPs within each of  
472 the two identified QTLs are highly associated with the observed variance in SKN-1  
473 requirement (Fig 5C; Supplementary Fig. 3C, D).

474 GWAS analysis on the *mom-2(RNAi)* phenotypic variation proved more challenging  
475 because this phenotype showed a highly skewed distribution (Shapiro-Wilk' test  $W = 0.8682$ ,  
476  $p\text{-value} = 1.207 \times 10^{-7}$ ) (Supplementary Fig. 4). Nevertheless, we applied a linear model GWAS  
477 adjusting the individual p-values using a permutation-based approach (see Materials and  
478 Methods) and EMMA (Fig. 5B, Supplementary Fig. 5A), which revealed highly correlated  
479 results among them (Pearson's  $R = 0.95$ ,  $p\text{-value} < 2.2 \times 10^{-16}$ ) (Supplementary Fig. 5B). Although  
480 GWAS identified 45 significant SNPs distributed across the genome (GWAS adjusted p-values  
481 < 0.01), EMMA did not reveal any significant genomic regions for *mom-2(RNAi)* variation  
482 based on FDR, suggesting that the MOM-2 requirement is a highly complex trait influenced



483 by many loci. However, when we compared the p-values of individual SNPs from *skn-1(RNAi)*  
 484 and *mom-2(RNAi)* EMMA, a substantial overlap in the central region of chromosome of  
 485 chromosome IV was observed (Supplementary Fig. 6). This genomic region showed striking  
 486 reciprocity in phenotype compared to the SKN-1 results, as described below.



487

488 **Fig. 5. Genome-Wide Association Studies of *skn-1(RNAi)* and *mom-2(RNAi)* phenotypes.**

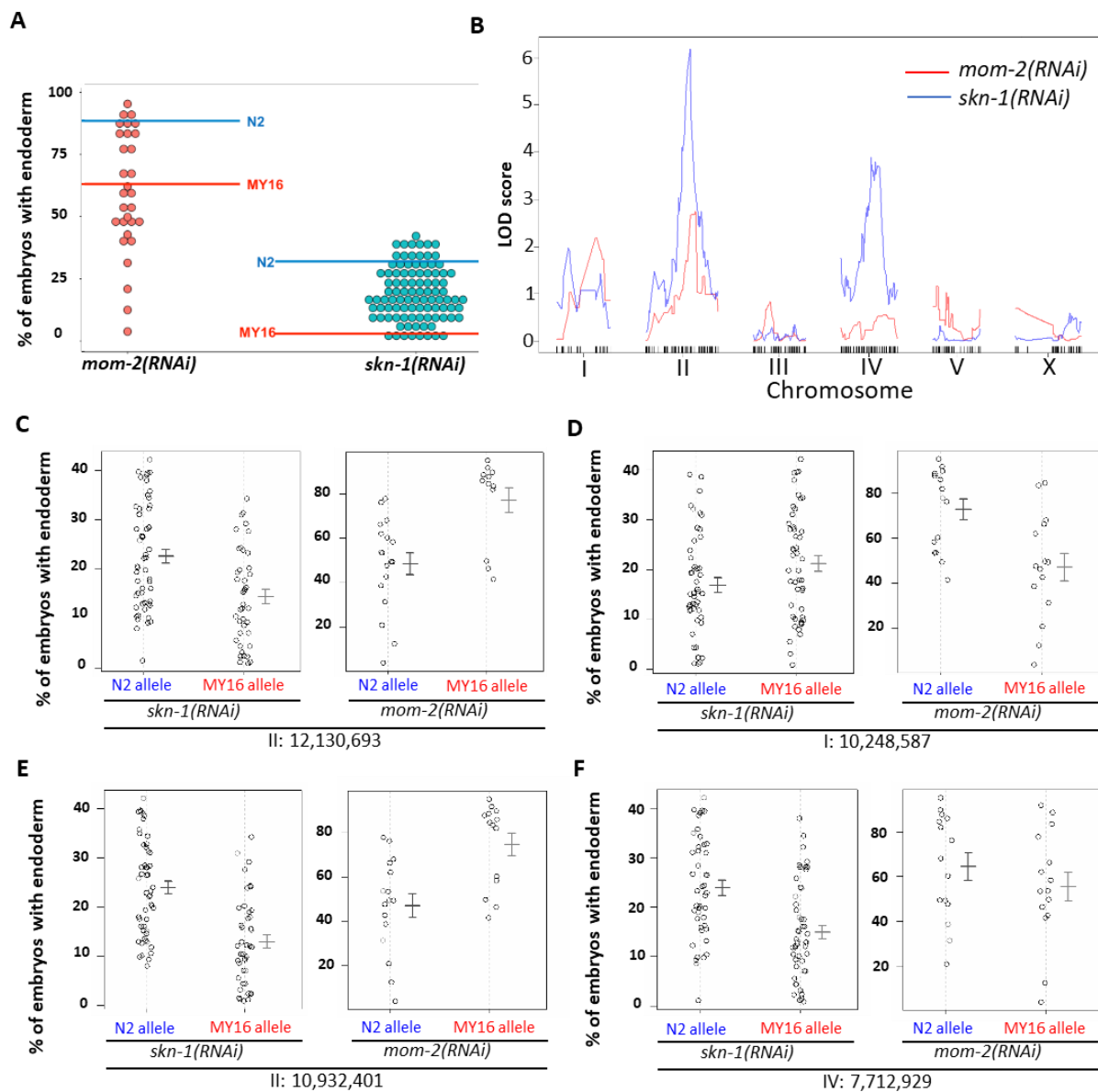
489 (A) Manhattan plot of *skn-1(RNAi)* EMMA. The red line indicates a genome-wide 1.5% FDR (permutation-  
 490 based FDR, from 10,000 permuted results). Black line represents 3.0% FDR. The y axis is the  $-\log_{10}$  of p-  
 491 value. (B) Manhattan plot of *mom-2(RNAi)* EMMA. The y axis is the  $-\log_{10}$  of p-value. Genomic regions  
 492 are shown on the x-axis. (C) Effect plots of the significant SNPs from *skn-1(RNAi)* GWAS (Suppl. Fig 3A) at  
 493 position 3,362,389 bp on chromosome I and position 17,924,783 bp on chromosome V (see Supplementary  
 494 Fig. 3). Horizontal lines within each box represent the median, and the boxes represent 25th–75th  
 495 percentile.

496 In an effort to narrow in on causal loci underlying the *skn-1(-)* and *mom-2(-)*  
 497 phenotypic variation, and to assess possible relationships between these two GRN inputs, we  
 498 prepared and analyzed 95 recombinant inbred lines (RILs) between two *C. elegans* isotypes,  
 499 N2 and MY16. These strains were chosen for their widely varying differences in requirement  
 500 for both SKN-1 and MOM-2 (see Materials and Methods). In contrast to the very low variation

501 seen between multiple trials of each parental strain, analysis of the RNAi treated RIL strains  
502 (>500 embryos/RIL) revealed a very broad distribution of phenotypes. We found that, while  
503 some RILs gave phenotypes similar to that of the two parents, many showed intermediate  
504 phenotypes and some were reproducibly more extreme than either parent, indicative of  
505 transgressive segregation [67]. For *skn-1(RNAi)*, the phenotype varied widely across the RILs,  
506 with 1 to 47% of embryos containing gut (Fig. 6A, Supplementary File 3). This effect was even  
507 more striking with *mom-2(RNAi)*, for which virtually the entire possible phenotypic spectrum  
508 was observed across a selection of 31 RILs representing the span of *skn-1(RNAi)* phenotypes.  
509 The *mom-2(RNAi)* phenotypes ranged from RILs showing 3% of embryos with gut to those  
510 showing 92% (Fig. 6A). It is noteworthy that one RIL (JR3572, Supplementary File 4) showed a  
511 nearly completely penetrant gutless phenotype, an effect that is much stronger than has been  
512 previously observed for *mom-2(-)* [29]. These results indicate that a combination of natural  
513 variants can nearly eliminate a requirement for MOM-2 altogether, while others make it  
514 virtually essential for endoderm development. Collectively, these analyses reveal that  
515 multiple quantitative trait loci (QTL) underlie SKN-1- and MOM-2-dependent endoderm  
516 specification.

517 To identify QTLs from the recombinant population, we performed linkage mapping for  
518 both phenotypes using both interval mapping and marker regression. For *skn-1(RNAi)*, two  
519 major peaks were revealed on chromosomes II and IV (above 1% FDR estimated from 1,000  
520 permutations). Two minor loci were found on chromosomes I and X (suggestive linkage,  
521 above 20% FDR) (Fig 6B). For *mom-2(RNAi)*, two major independent QTL peaks were found  
522 on Chromosomes I and II (above the 5% FDR estimated from 1,000 permutations). Although  
523 the candidate peaks observed on Chromosome IV for *skn-1(RNAi)* (Fig. 6B) did not appear to  
524 overlap with those for *mom-2(RNAi)*, overlap was observed between the Chromosomes I and

525 II candidate regions for these two phenotypes. Moreover, many N2 and MY16 alleles in the  
 526 QTL showed a reciprocal effect on SKN-1 and MOM-2 dependence (Fig. 6C-F).



527  
 528 **Fig 6. Quantitative genetic analysis of *mom-2(RNAi)* and *skn-1(RNAi)* phenotype in Recombinant Inbred**  
 529 **Lines (RILs) between N2 and MY16.**

530 (A) *mom-2(RNAi)* (left) and *skn-1(RNAi)* (right) phenotype of RILs. The phenotype of the parental strains,  
 531 MY16 and N2 are shown by red and blue lines, respectively. (B) QTL analyses (interval mapping) of *skn-*  
 532 *1(RNAi)* (blue line) and *mom-2(RNAi)* (red line) phenotype shown in (A). Genomic regions are shown on the  
 533 x-axis and LOD score is shown on the y-axis. (C-F) Effect plots of significant SNPs from *mom-2(RNAi)* (C, D)  
 534 and *skn-1(RNAi)* (E, F) QTL analyses of RILs. Each dot represents a RIL. The parental alleles are shown on  
 535 the x-axis, and *skn-1(RNAi)* or *mom-2(RNAi)* phenotypes on the y-axis. Confidence intervals for the average  
 536 phenotype in each genotype group are shown.

537

538 **A cryptic compensatory relationship between the SKN-1 and Wnt regulatory inputs**

539

540 As with *skn-1(RNAi)* findings, we found no correlation between the *mom-2(RNAi)* phenotype

541 and phylogenetic relatedness or geographical distribution (Supplementary Fig. 7), suggesting

542 rapid intraspecies developmental system drift. This, together with the preceding findings,

543 unveiled wide cryptic variation in the requirements for both SKN-1 and MOM-2/Wnt in the

544 endoderm GRN and raised the possibility of a functional overlap in this variation. Comparisons

545 of the GWAS and QTL mapping results for *skn-1* and *mom-2* showed an overlap in candidate

546 QTL regions on chromosome I, II and IV (Fig. 5, Fig 6, Supplementary Fig. 6), suggesting a

547 possible relationship between the genetic basis underlying these two traits. It is conceivable

548 that some genetic backgrounds are generally more sensitive to loss of either input (e.g, the

549 threshold for activating the GRN is higher) and others more robust to single-input loss.

550 Alternatively, a higher requirement for one input might be associated with a relaxed

551 requirement for the other, i.e., a reciprocal relationship.

552 As an initial assessment of these alternatives, we examined whether the requirements

553 for SKN-1 and MOM-2 across all strains were significantly correlated. This analysis revealed

554 no strong relationship between the cryptic variation in the requirement for these inputs seen

555 across all the strains (Spearman correlation  $R=0.18$ ,  $p\text{-value}=0.07$ ) (Fig. 7A). This apparent lack

556 of correlation at the level of strains is not unexpected, as many factors likely contribute to the

557 cryptic variation and the comparison reflects the collective effect of all causal loci in the

558 genome of each strain.

559 We next sought to examine possible relationships between the two GRN inputs at

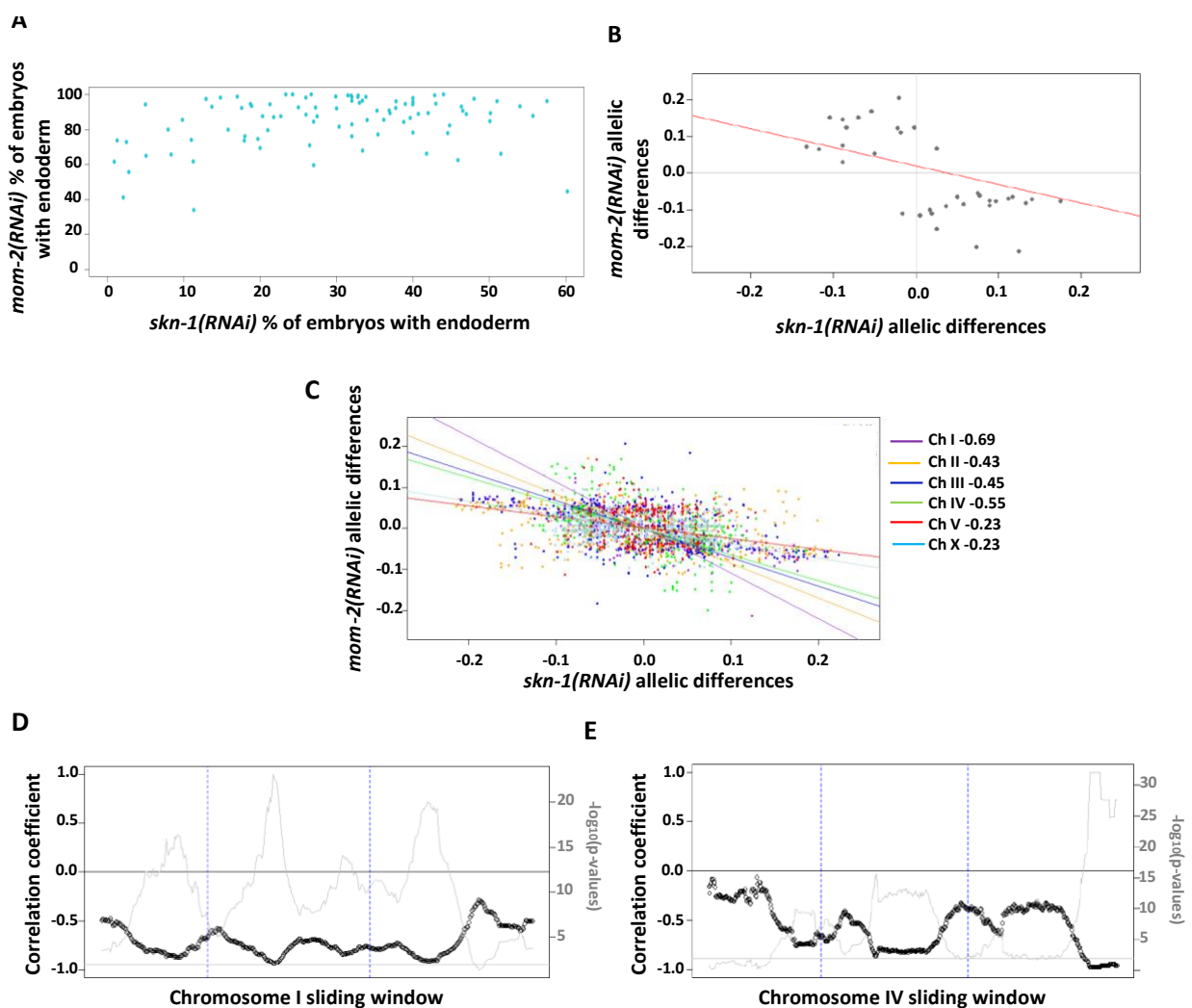
560 higher resolution by comparing association of specific genetic regions with the quantitative

561 requirement for each input. We took advantage of the available sequence data for all the

562 isotypes tested [40] and examined the impact of each allele on the *skn-1(RNAi)* and *mom-*  
563 *2(RNAi)* phenotypes for the SNPs that were most highly associated with the variation in  
564 requirement for SKN-1 by calculating the difference between the phenotypic medians for  
565 each allele at each SNP. Comparisons of the GWAS analyses for variation in the requirement  
566 for SKN-1 and MOM-2 showed a particularly strong overlap in candidate QTL regions for the  
567 two phenotypes on chromosome IV (Fig. 5A, B, Supplementary Fig. 3A, 5, 6). To assess the  
568 relationship between these and other significant SNPs, we analyzed the top 45 SNPs from the  
569 *mom-2* GWAS/EMMA data and found a strong negative correlation between the allelic effects  
570 for SKN-1 and MOM-2 dependence. With very few exceptions, SNPs associated with a milder  
571 *skn-1(RNAi)* phenotype (higher % with endoderm) showed a stronger *mom-2(RNAi)*  
572 phenotype (low %) and *vice versa* (Fig. 7B), with an overall highly significant negative  
573 correlation (Pearson's correlation  $R=-0.6099$ ,  $p\text{-value}=0.0001$ ).

574         The strong negative correlation we observed between the strength of the *skn-1(RNAi)*  
575 and *mom-2(RNAi)* phenotypes for the SNPs that are most significantly associated with the  
576 variation might be explained in part by the large blocks of linkage disequilibrium observed in  
577 *C. elegans* [40]. Thus, in principle, relatively few genomic regions might, by chance, show the  
578 reciprocal relationship, in which case all linked high-significance SNPs would similarly show  
579 the negative correlation. It was therefore important to assess how widespread and consistent  
580 this effect is across the entire genome. We dissected the relationship of the SKN-1 and MOM-  
581 2 requirements across all chromosomes by analyzing the phenotypic strength in sliding  
582 windows of 50 SNPs each across each chromosome, using all 4,690 SNPs. This analysis  
583 revealed a striking overall trend: for all six chromosomes, regions associated with high SKN-1  
584 requirement showed a tendency toward lower MOM-2/Wnt requirement and *vice-versa*. This  
585 effect was most pronounced on chromosome I, which showed a very strong negative

586 correlation ( $R=-0.69$ ). The effect was also clearly evident on chromosomes IV ( $R=-0.55$ ), III ( $R=-$   
587  $0.45$ ), and II ( $R=-0.43$ ). Though weaker for chromosomes V and X ( $R=-0.23$  for both), the  
588 correlation was nonetheless negative for these chromosomes as well (Fig. 7C-E;  
589 Supplementary Fig. 8A-E). Thus, the inverse relationship between the MOM-2 and SKN-1  
590 requirement appears to be distributed across the entire genome. The sequences underlying  
591 the cryptic variation we observed might not be expected to be uniformly distributed  
592 throughout the genome and, indeed, we found that strength of the correlation varied widely  
593 between and even within chromosomes (Fig. 7C-E, Supplementary Fig. 8B-E).



595 **Fig. 7: Negative correlation of *skn-1(RNAi)* and *mom-2(RNAi)* allelic differences.**

596 (A) Comparison of *skn-1(RNAi)* and *mom-2(RNAi)* phenotype in 94 strains tested. No correlation was found  
597 (Spearman correlation  $R=0.1844$ ,  $p\text{-value}=0.07$ ). Each dot corresponds to a wild isolate. Y-axis, *skn-1(RNAi)*  
598 phenotype, x-axis, *mom-2(RNAi)* phenotype. (B) Negative correlation of *skn-1(RNAi)* and *mom-2(RNAi)*  
599 allelic differences at the top SNPs from the *mom-2(RNAi)* GWAS as calculated by subtracting the median  
600 (of the *skn-1(RNAi)* and *mom-2(RNAi)* phenotypes) of one allele to the median of the second. Pearson's  
601 correlation  $R=-0.6099$ ,  $p\text{-value}=0.0001$ . (C) Genome-wide negative correlation in allelic effects. Each dot  
602 represents a SNP, and 4,690 SNPs in total were analyzed. The chromosomes and their corresponding  
603 regression lines are color-coded. The R-value of each chromosome is indicated. Correlation sliding window  
604 of (D) chromosome I and (E) chromosome IV. Windows of 50 SNPs were used to calculate the correlation  
605 coefficient and p-value. Black circles represent the correlation coefficient (R value) for each window (scale  
606 on the x-axis). Black line indicates the 0 threshold. Grey line represents the  $-\log_{10}$  of the p-values for the  
607 corresponding correlation windows (scale on the y-axis). Grey horizontal line is the significance threshold  
608 set at  $p\text{-value}=0.01$ . Blue dotted lines divide chromosomal region into left, middle and right arms.

### 609 **Multiple factors reciprocally regulate the requirement for SKN-1 and MOM-2/Wnt**

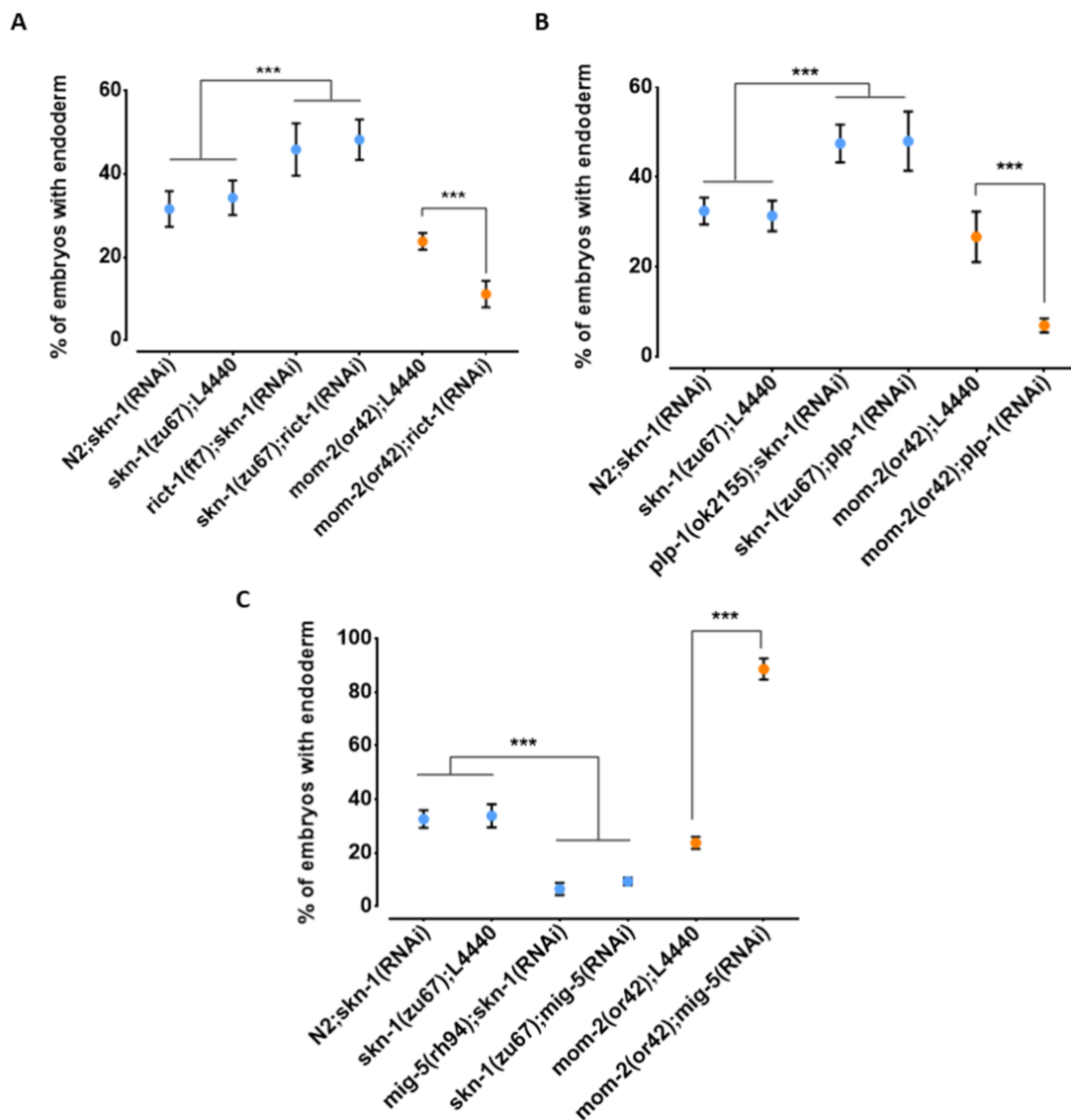
610 We further explored this relationship between the requirement for SKN-1 and MOM-  
611 2 by testing other candidate genes implicated in endoderm development [68–70]. We found  
612 that loss of RICT-1, the *C. elegans* orthologue of the human RICTOR (Rapamycin-insensitive  
613 companion of mTOR; [71]), a component of the TORC2 complex, which has been shown to  
614 antagonize SKN-1 function [68], results in opposite effects on *skn-1(-)* and *mom-2(-)* mutants  
615 (Fig. 8A). Specifically, while *ric1-1(RNAi)* suppresses the absence of gut in *skn-1(zu67)* embryos  
616 (*skn-1(zu67)*: 34.3%  $\pm$  s.d 4.1% with gut vs. *skn-1(zu67); ric1-1(RNAi)*: 48.3%  $\pm$  s.d 4.9%;  
617  $p<0.001$ ), we found that it *enhances* this phenotype in *mom-2(or42)* mutants (*mom-2(or42)*:  
618 23.8%  $\pm$  s.d 2.0%; vs. *mom-2(or42); ric1-1(RNAi)*: 11.2%  $\pm$  s.d 3.2%;  $p<0.001$ ). Confirming this  
619 effect, a similar outcome was observed when SKN-1 was depleted by RNAi in *ric1-1(ft7)*  
620 chromosomal mutants (*skn-1(RNAi)*: 31.6%  $\pm$  s.d 4.3% with gut vs. *ric1-1(ft7); skn-1(RNAi)*:  
621 45.9%  $\pm$  s.d 6.3%;  $p<0.05$ ) (Fig. 8A). Similarly, RNAi depletion of PLP-1, the *C. elegans*  
622 homologue of the Pur alpha transcription factor that has been shown to bind to and regulate  
623 the *end-1* promoter [69], reciprocally affects the outcome of removing these two inputs in  
624 the same direction: loss of PLP-1 function suppresses the *skn-1(-)* phenotype (to 48.0%  $\pm$  s.d  
625 6.6%), and strongly enhances the *mom-2* phenotype (to 6.9%  $\pm$  s.d 1.6%). Again, this result

626 was confirmed by RNAi of *skn-1* in a *plp-1(ok2156)* chromosomal mutant (Fig. 8B). Thus, as  
627 observed with the effect across the genome with natural variants, we observed a striking  
628 reciprocal effect of both of these genes on loss of SKN-1 and MOM-2.

629 We also observed a reciprocal effect on the SKN-1 and Wnt inputs with MIG-  
630 5/*dishevelled*, a component of the Wnt pathway that acts downstream of the Wnt receptor  
631 [70]; however, in this case the effect was in the opposite direction as seen for RICT-1 and PLP-  
632 1. Loss of MIG-5 as a result of chromosomal mutation or RNAi leads to *enhancement* of the  
633 *skn-1(-)* phenotype (*mig-5(rh94); skn-1(RNAi)*: 6.6%  $\pm$  s.d 2.3%; *skn-1(zu67); mig-5(RNAi)*:  
634 9.4%  $\pm$  s.d 1.4%) and *suppression* of the *mom-2(-)* phenotype (88.6%  $\pm$  s.d 4.0%) (Fig 8C).

635 Together, these findings reveal that, as observed with the natural variant alleles  
636 (Fig.5C, Fig. 6C-F; Fig. 7B, C), RICT-1, PLP-1, and MIG-5 show opposite effects on the  
637 phenotype of removing SKN-1 and MOM-2, suggesting a prevalence of genetic influences that  
638 reciprocally influence the outcome in the absence of these two inputs.





639

640 **Fig 8. Reciprocal effects of RICT-1, PLP-1, and MIG-5 on *skn-1(-)* and *mom-2(-)* phenotypes**

641 (A, B) Loss of RICT-1 or PLP-1 enhances the *mom-2(or42)* loss-of-endoderm phenotype and suppresses  
 642 *skn-1(zu67)* and *skn-1(RNAi)* phenotype. (C) Loss of MIG-5 enhances the *skn-1(zu67)* and *skn-1(RNAi)*  
 643 phenotype and suppresses *mom-2(or42)* phenotype. At least three replicates were performed per  
 644 experiment. Student t-test (\*\*\*) p-value<0.001). Data represented with Standard Deviations.

645

## 646 DISCUSSION

647           The remarkable variety of forms associated with the ~36 animal phyla [72] that  
648 emerged from a common metazoan ancestor >600 Mya is the product of numerous  
649 incremental changes in GRNs underlying the formation of the body plan and cell types. Here,  
650 we describe an unexpectedly broad divergence in the deployment of SKN-1/Nrf and MOM-  
651 2/Wnt signaling in generating the most ancient germ layer, the endoderm, within wild isolates  
652 of a single animal species, *C. elegans*. In this study, we report five major findings: 1) while the  
653 quantitative requirement for two distinct regulatory inputs that initiate expression of the  
654 endoderm GRN (SKN-1 and MOM-2) are highly reproducible in individual *C. elegans* isolates,  
655 there is wide cryptic variation between isolates. 2) Cryptic variation in the requirement for  
656 these regulatory factors shows substantial differences even between closely related strains,  
657 suggesting that these traits are subject to rapid evolutionary change in this species. 3)  
658 Quantitative genetic analyses of natural and recombinant populations revealed multiple loci  
659 underlying the variation in the requirement for SKN-1 and MOM-2 in endoderm specification.  
660 4) The quantitative requirements for SKN-1 and MOM-2 in endoderm specification are  
661 negatively correlated across the genome, as shown by allelic effect analysis, implying a  
662 reciprocal requirement for the two inputs. 5) *rict-1*, *plp-1*, and *mig-5* reciprocally influence  
663 the outcome of *skn-1(-)* and *mom-2(-)*, substantiating the reciprocal influences on the two  
664 GRN inputs. These findings reveal substantial plasticity and complexity underlying SKN-1 and  
665 MOM-2/Wnt regulatory inputs in mobilizing a conserved system for endoderm specification.

666           Together, these findings indicate that, while the core genetic toolkit for the  
667 development of the endoderm, the most ancient of the three germ layers, appears to have  
668 been preserved for well over half a billion years, the molecular regulatory inputs that initiate

669 its expression in *C. elegans* vary extremely rapidly over short evolutionary time scales within  
670 the species.

### 671 **Evolutionary plasticity in maternal regulators of embryonic GRNs**

672 The finding that the key regulatory inputs that initiate the endoderm GRN show  
673 dramatic plasticity is in accordance with the “hourglass” concept of embryonic development  
674 [73–75], in which divergent developmental mechanisms converge on a more constant state  
675 (i.e., a “phylotypic stage” at the molecular regulatory level). Indeed, it appears that a  
676 downstream GATA factor cascade that directs endoderm specification and differentiation is  
677 a highly conserved feature not only across *Caenorhabditis* species [38,76,77] but, in fact, across  
678 the broad spectrum of animal phyla [12–17]. These observations are also consistent with the  
679 notion that, while the late stages in organ differentiation involve activation of a very large  
680 number of target differentiation genes by a limited set of transcription factors, thereby  
681 restricting evolutionary divergence at that stage in the regulatory circuitry, the early stages  
682 involve the action of transcription factors on far fewer target genes, hence allowing for much  
683 greater evolutionary plasticity [21].

684 In *Drosophila*, early maternally acting genes show more rapid evolution than those  
685 expressed zygotically [78]. Moreover, maternal patterning systems that spatially regulate  
686 conserved patterning gene networks between broadly divergent insect species are highly  
687 divergent [79,80]. Further comparisons of early embryonic transcripts across many  
688 *Drosophila* species and *Aedes aegypti* revealed that maternal transcript pools that, like those  
689 of *C. elegans skn-1*, are present only transiently during early embryogenesis, and expression  
690 levels are highly variable across these species, spanning ~60 My of evolution [81]. What is  
691 particularly striking about our findings is that the varying requirement for key maternal

692 regulatory components is seen within the relatively recent radiation of a single species with  
693 low genetic diversity [40]. Variation in gene expression predicts phenotypic severity of  
694 mutations in different genetic backgrounds [82]. As quantitative transcriptional profiling of *C.*  
695 *elegans* isotypes advances, it will be of interest to assess whether the highly evolvable  
696 requirement for maternal regulatory inputs into the endoderm GRN similarly correlates with  
697 rapid divergence in quantitative levels of maternal transcripts that are transiently deployed  
698 in early embryos of this species.

### 699 **Multigenic variation in the requirement for SKN-1 and MOM-2**

700 GWAS and EMMA revealed several major candidate QTLs (Fig. 5, Supplementary Fig.  
701 3, 5), implying that multigenic factors are causally responsible for the differences in  
702 requirement for SKN-1 and MOM-2 between isotypes. This multigenic influence was also  
703 apparent from analysis of RILs derived from N2 and MY16 parental strains, which identified  
704 several loci associated with both traits. In addition, we found substantial epistasis between  
705 the different genomic regions underlying this variation. Transgressive segregation of the  
706 requirement for both SKN-1 and MOM-2 was seen in the RIL sets (Fig. 6A). For example, the  
707 MY16 strain which shows an almost fully penetrant requirement for SKN-1 for gut  
708 development, appears to harbor cryptic variants that suppress the requirement for SKN-1,  
709 allowing enhanced gut development when combined with genetic factors in the N2 strain.

710 We observed substantial overlap on chromosome IV in the GWAS/EMMA analyses of  
711 the *skn-1* and *mom-2* requirements in wild isotypes (Fig. 5, Supplementary Fig. 6) and on  
712 chromosome II from analyses using RILs (Fig. 6B). This finding raises the possibility that some  
713 QTLs may influence requirement for both inputs into the endoderm specification pathway: as  
714 SKN-1 and Wnt converge to regulate expression of the *end-1/3* genes, it is conceivable that

715 common genetic variants might modulate the relative strength or outcome of both maternal  
716 inputs. However, our findings do not resolve whether these genetic variants act  
717 independently to influence the maternal regulatory inputs.

718 Genetic interactions are often neglected in large-scale genetic association studies [83]  
719 owing in part to the difficulty in confirming them [84]. Many studies [85–88], including ours  
720 here, showed that epistasis can strongly influence the behavior of certain variants upon  
721 genetic perturbation. In addition, selection on pleiotropically acting loci facilitates rapid  
722 developmental system drift [87,89,90]. Together, epistasis and selection on pleiotropic loci  
723 play important roles in the evolution of natural populations [89–92].

#### 724 **Potential compensatory relationships between SKN-1 and MOM-2/Wnt**

725 Although we did not observe a direct correlation between the *skn-1(-)* and *mom-2(-)*  
726 phenotypes across the isotypes studied here, a clear inverse correlation was observed when  
727 testing associated individual SNPs in significantly linked loci (Fig. 7). This reciprocal effect seen  
728 across large portions of the genome may be attributable in part to the large LD blocks present  
729 on all chromosomes (Fig. 7, Supplementary Fig. 8) [40]. However, our finding that this effect  
730 is seen across the entire genome raises the possibility that the SKN-1 and MOM-2/Wnt inputs  
731 might compensate for each other and that genetic variants that enhance the requirement for  
732 one of the inputs relaxes the requirement for the other. This reciprocity might reflect cross-  
733 regulatory interactions between these two maternal inputs or may be the result of  
734 evolutionary constraints imposed by selection on these genes, which act pleiotropically in a  
735 variety of processes.

736 We identified two genes, *rict-1* and *plp-1*, that show similar inverse effects on the  
737 requirements from *skn-1* and *mom-2*: debilitation of either gene enhances the phenotype of

738 *mom-2(-)* and suppresses that of *skn-1(-)*. RICT-1 function extends lifespan in *C. elegans*  
739 through the action of SKN-1 [68], and loss of RICT-1 rescues the misspecification of the MS  
740 and E blastomeres and lethality of *skn-1(-)* embryos [68], consistent with our finding.  
741 However, the mechanism by which loss of *rict-1* synergizes with a defect in the Wnt pathway  
742 is not clear. We previously showed that PLP-1, a homologue of the vertebrate transcription  
743 factor pur alpha, binds to the *end-1* promoter and acts in parallel to the Wnt pathway and  
744 downstream of the MAPK signal [69], thereby promoting gut formation. PLP-1 shows a similar  
745 reciprocal relationship with SKN-1 and MOM-2 as with RICT-1 (Fig. 8). Given that PLP-1 binds  
746 at a *cis* regulatory site in *end-1* near a putative POP-1 binding site [69], and that SKN-1 also  
747 binds to the *end-1* regulatory region [64], it is conceivable that this reciprocity reflects  
748 integration of information at the level of transcription factor binding sites. As the architecture  
749 of the GRN is shaped by changes in *cis*-regulatory sequences [1,3], analyzing alterations in  
750 SKN-1 and Wnt/POP-1 targets among *C. elegans* wild isolates may provide insights into how  
751 genetic changes are accommodated without compromising the developmental output at  
752 microevolutionary time scale.

753         MIG-5, a *dishevelled* orthologue, functions in the Wnt pathway in parallel to Src  
754 signaling to regulate asymmetric cell division and endoderm induction [28,70]. We found that  
755 the loss of *mig-5* function enhances the gut defect of *skn-1(-)* and suppresses that of the *mom-*  
756 *2(-)*, the opposite reciprocal relationship to that of *rict-1* and *plp-1*, and consistent with a  
757 previous report (Fig. 8) [28]. These effects were not observed in embryos lacking function of  
758 *dsh-2*, the orthologue of *mig-5* (data not shown), supporting a previous study that showed  
759 overlapping but non-redundant roles of MIG-5 and DSH-2 in EMS spindle orientation and gut  
760 specification [70]. Recent studies showed that Dishevelled can play both positive and negative  
761 roles during axon guidance [93,94]. Dishevelled, upon Wnt-activation, promotes

762 hyperphosphorylation and inactivation of Frizzled receptor to fine-tune Wnt activity. It is  
763 tempting to speculate that MIG-5 may perform similar function in EMS by downregulating  
764 activating signals (Src or MAPK), in the absence of MOM-2.

765 We hypothesize that compensatory mechanisms may evolve to fine-tune the level of  
766 gut-activating regulatory inputs. Successful developmental events depend on tight spatial and  
767 temporal regulation of gene expression. For example, anterior-posterior patterning in the  
768 *Drosophila* embryo is determined by the local concentrations of the Bicoid, Hunchback, and  
769 Caudal transcription factors [95]. We postulate that SKN-1 and Wnt signaling is modulated so  
770 that the downstream genes, *end-1/3*, which control specification and later differentiation of  
771 endoderm progenitors, are expressed at optimal levels that ensure normal gut development.  
772 Suboptimal END activity leads to poorly differentiated gut and both hypo- and hyperplasia in  
773 the gut lineage [96–98]. Hyper- or hypo-activation of Wnt signaling has been implicated in  
774 cancer development [99], bone diseases [100,101], and metabolic diseases [102,103],  
775 demonstrating the importance of regulating the timing and dynamics of such developmental  
776 signals within a quantitatively restricted window.

### 777 **Cryptic variation and evolvability of GRNs**

778 This study revealed substantial cryptic genetic modifications that alter the relative  
779 importance of two partially redundant inputs into the *C. elegans* endoderm GRN, leading to  
780 rapid change in the developmental network architecture (Fig. 9). Such modifications may  
781 occur through transitional states that are apparent even within the radiation of this single  
782 species. For example, the finding that POP-1 is not required for gut development even in a  
783 wild isolate (e.g., MY16) that, like *C. briggsae*, shows a near-absolute requirement for SKN-1  
784 may reflect a transitional state between the two species: *i.e.*, a nearly essential requirement

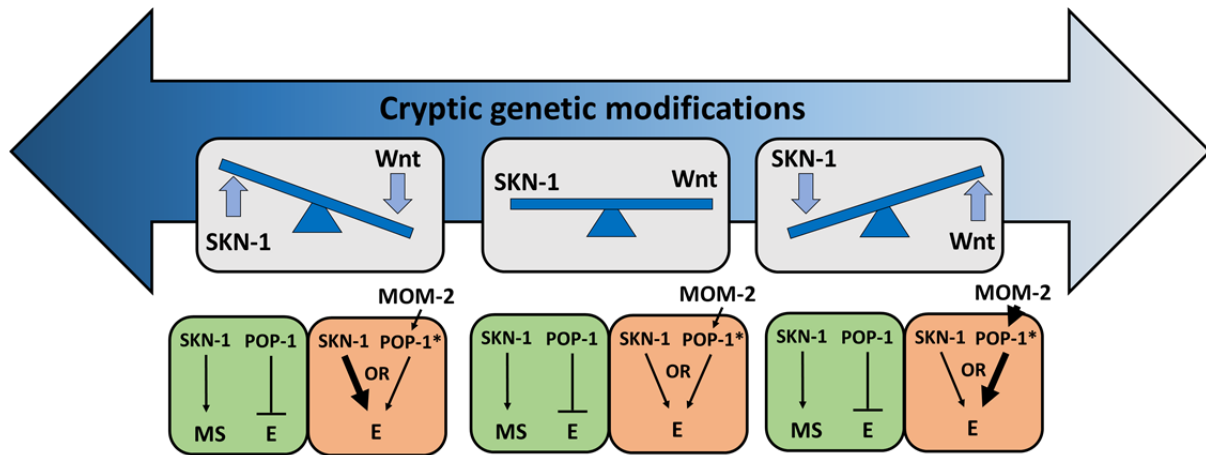
785 for SKN-1 but non-essential requirement for POP-1, an effect not previously seen in either  
786 species. In addition, duplicated GATA factors (the MEDs, ENDS, and ELTs) and partially  
787 redundant activating inputs (SKN-1, Wnt, Src, and MAPK) in endoderm GRN, provide an  
788 opportunity for genetic variation to accumulate and “experimentation” of new regulatory  
789 relationships without diminishing fitness [2,104,105].

790 Redundancy in the system may act to ‘rescue’ an initial mutation and allow for  
791 secondary mutations that might eventually lead to rewiring of the network. For example, loss  
792 of either MyoD or Myf5, two key regulators of muscle differentiation in metazoans, produces  
793 minimal defects in myogenesis as a result of compensatory relationship between the  
794 myogenic factors [106]. In vertebrates, gene duplication events have resulted in an expansion  
795 of Hox genes to a total of >200, resulting in prevalent redundancy [107–109]. This  
796 proliferation of redundant genes provides opportunities for evolutionary experimentation  
797 and subsequent specialization of new functions [109]. In *C. elegans*, loss of GAP-1 (a Ras  
798 inhibitor) or SLI-1 (a negative regulator of EGFR signaling) alone does not produce obvious  
799 defects, while double mutations lead to a multivulva phenotype [110]. Many other similar  
800 redundant relationships between redundant partners exist in the animal. Notably, the relative  
801 importance of Ras, Notch, and Wnt signals in vulva induction differ in various genetic  
802 backgrounds [6,65] and physiological conditions [111,112], resulting in flexibility in the  
803 system. While vulval development in *C. elegans*, when grown under standard laboratory  
804 conditions, predominantly favors utilization of the EGF/Ras signaling pathway [111], Wnt is  
805 the predominant signaling pathway in the related *Pristionchus pacificus*, which is ~250 MY  
806 divergent [113]. In addition, while *Cel-lin-17* functions positively to transduce the Wnt signal,  
807 *Ppa-lin-17/Fz* antagonizes Wnt signaling and instead the Wnt signal is transmitted by *Ppa-lin-*  
808 *18/Ryk*, which has acquired a novel SH3 domain not present in the *C. elegans* ortholog [114].



809 Thus, extensive rewiring of signaling networks and modularity of signaling motifs contribute  
810 to developmental systems drift.

811 The broad cryptic variation we have observed in this study may drive developmental  
812 system drift, giving rise to GRN architectures that differ in the relative strength of the network  
813 components. In the developmental hourglass model of evolvability of animal development,  
814 the early stages of embryonic development showed the least constraint in gene expression  
815 compared to either the phylotypic stage or post phylotypic stage. This is likely attributable  
816 either to positive selection during early embryonic and later larval stages or to developmental  
817 constraints. Analysis of developmental gene expression in mutation accumulation lines,  
818 which have evolved in the absence of any positive selection, showed similarity to the  
819 developmental hourglass model of evolvability, consistent with strong developmental  
820 constraints on the phylotypic stage [115]. However, they do not rule out the possibility that  
821 early and late stages of development might be more adaptive and therefore subject to  
822 positive selection. It will be of interest to learn the degree to which the divergence in network  
823 architecture might arise as a result of differences in the environment and selective pressures  
824 on different *C. elegans* isotypes.



825

826 **Fig. 9. Simplified models accounting for cryptic compensatory relationship between the SKN-1 and**  
827 **MOM-2/Wnt regulatory inputs in the endoderm GRN.**

828 Accumulation of cryptic genetic modifications drives rapid rewiring of the GRN, causing broad variation of  
829 SKN-1 and MOM-2/Wnt dependence in endoderm (E) specification among *C. elegans* isotypes. Wnt-  
830 signaled POP-1 (indicated by \*) acts as an E activator, while unmodified POP-1 in the MS blastomere acts  
831 as a repressor of E fate in all *C. elegans* isotypes. The relative strength of the inputs is indicated by the  
832 thickness of the arrow.

833 **ACKNOWLEDGMENTS**

834 We thank members of the Rothman, especially Sagen Flowers and Kristoffer C. Mellinger for  
835 experimental assistance, and Snell labs, particularly Dr. Kien Ly, for helpful advice and  
836 feedback. We thank Dr. Kathy Ruggiero (University of Auckland, New Zealand) for helpful  
837 advice on GWAS methodology and Dr. James McGhee (University of Calgary, Canada) for  
838 providing the MH33 antibody. Nematode strains used in this work were provided by the  
839 Caenorhabditis Genetics Center, which is funded by the National Institutes of Health - Office  
840 of Research Infrastructure Programs (P40 OD010440). Y.N.T.C was supported during part of  
841 this work by a University of Auckland Doctoral Scholarship. This work was supported by grants  
842 from the NIH (#1R01HD082347 and # 1R01HD081266) to J.H.R.

843 **COMPETING INTERESTS**

844 The authors declare no competing or financial interests.

845 **REFERENCES**

- 846 1. Peter IS, Davidson EH. Evolution of gene regulatory networks controlling body plan  
847 development. *Cell*. Elsevier; 2011;144: 970–85. doi:10.1016/j.cell.2011.02.017
- 848 2. Félix M-A, Wagner A. Robustness and evolution: concepts, insights and challenges  
849 from a developmental model system. *Heredity (Edinb)*. Nature Publishing Group;  
850 2008;100: 132–140. doi:10.1038/sj.hdy.6800915
- 851 3. Davidson EH, Levine MS. Properties of developmental gene regulatory networks. *Proc*  
852 *Natl Acad Sci U S A*. National Academy of Sciences; 2008;105: 20063–6.  
853 doi:10.1073/pnas.0806007105
- 854 4. Oliveri P, Tu Q, Davidson EH. Global regulatory logic for specification of an embryonic  
855 cell lineage. *Proc Natl Acad Sci U S A*. National Academy of Sciences; 2008;105: 5955–  
856 62. doi:10.1073/pnas.0711220105
- 857 5. Peter IS, Davidson EH. Assessing regulatory information in developmental gene  
858 regulatory networks. *Proc Natl Acad Sci U S A*. National Academy of Sciences;  
859 2017;114: 5862–5869. doi:10.1073/pnas.1610616114
- 860 6. Milloz J, Duveau F, Nuez I, Felix M-A. Intraspecific evolution of the intercellular  
861 signaling network underlying a robust developmental system. *Genes Dev*. 2008;22:  
862 3064–3075. doi:10.1101/gad.495308
- 863 7. Nunes MDS, Arif S, Schlötterer C, McGregor AP. A perspective on micro-evo-devo:  
864 progress and potential. *Genetics*. *Genetics*; 2013;195: 625–34.  
865 doi:10.1534/genetics.113.156463
- 866 8. Phinchongsakuldit J, MacArthur S, Brookfield JFY. Evolution of Developmental Genes:

- 867 Molecular Microevolution of Enhancer Sequences at the Ubx Locus in *Drosophila* and  
868 Its Impact on Developmental Phenotypes. *Mol Biol Evol.* 2003;21: 348–363.  
869 doi:10.1093/molbev/msh025
- 870 9. Hashimshony T, Feder M, Levin M, Hall BK, Yanai I. Spatiotemporal transcriptomics  
871 reveals the evolutionary history of the endoderm germ layer. *Nature.* Nature  
872 Publishing Group; 2015;519: 219–222. doi:10.1038/nature13996
- 873 10. Rodaway A, Patient R. Mesendoderm: An Ancient Germ Layer? *Cell.* Cell Press;  
874 2001;105: 169–172. doi:10.1016/S0092-8674(01)00307-5
- 875 11. Peterson KJ, Lyons JB, Nowak KS, Takacs CM, Wargo MJ, McPeck MA. Estimating  
876 metazoan divergence times with a molecular clock. *Proc Natl Acad Sci U S A.* National  
877 Academy of Sciences; 2004;101: 6536–41. doi:10.1073/pnas.0401670101
- 878 12. Martindale MQ, Pang K, Finnerty JR. Investigating the origins of triploblasty:  
879 “mesodermal” gene expression in a diploblastic animal, the sea anemone  
880 *Nematostella vectensis* (phylum, Cnidaria; class, Anthozoa). *Development.* The  
881 Company of Biologists Ltd; 2004;131: 2463–74. doi:10.1242/dev.01119
- 882 13. Boyle MJ, Seaver EC. Developmental expression of *foxA* and *gata* genes during gut  
883 formation in the polychaete annelid, *Capitella* sp. I. *Evol Dev.* 2008;10: 89–105.  
884 doi:10.1111/j.1525-142X.2007.00216.x
- 885 14. Boyle MJ, Seaver EC. Expression of *FoxA* and *GATA* transcription factors correlates  
886 with regionalized gut development in two lophotrochozoan marine worms:  
887 *Chaetopterus* (Annelida) and *Themiste lageniformis* (Sipuncula). *Evodevo.* 2010;1: 2.  
888 doi:10.1186/2041-9139-1-2

- 889 15. Gillis WJ, Bowerman B, Schneider SQ. Ectoderm- and endomesoderm-specific GATA  
890 transcription factors in the marine annelid *Platynereis dumerilli*. *Evol Dev.* 2007;9:  
891 39–50. doi:10.1111/j.1525-142X.2006.00136.x
- 892 16. Davidson EH, Rast JP, Oliveri P, Ransick A, Calestani C, Yuh C-H, et al. A Provisional  
893 Regulatory Gene Network for Specification of Endomesoderm in the Sea Urchin  
894 Embryo. *Dev Biol.* 2002;246: 162–190. doi:10.1006/dbio.2002.0635
- 895 17. Shoichet SA, Malik TH, Rothman JH, Shivdasani RA. Action of the *Caenorhabditis*  
896 *elegans* GATA factor END-1 in *Xenopus* suggests that similar mechanisms initiate  
897 endoderm development in ecdysozoa and vertebrates. *Proc Natl Acad Sci U S A.*  
898 National Academy of Sciences; 2000;97: 4076–81. Available:  
899 <http://www.ncbi.nlm.nih.gov/pubmed/10760276>
- 900 18. Sulston JE, Schierenberg E, White JG, Thomson JN. The embryonic cell lineage of the  
901 nematode *Caenorhabditis elegans*. *Dev Biol.* 1983;100: 64–119. Available:  
902 <http://www.ncbi.nlm.nih.gov/pubmed/6684600>
- 903 19. Bowerman B, Eaton BA, Priess JR. *skn-1*, a maternally expressed gene required to  
904 specify the fate of ventral blastomeres in the early *C. elegans* embryo. *Cell.* 1992;68:  
905 1061–75. Available: <http://www.ncbi.nlm.nih.gov/pubmed/1547503>
- 906 20. Bowerman B, Draper BW, Mello CC, Priess JR. The maternal gene *skn-1* encodes a  
907 protein that is distributed unequally in early *C. elegans* embryos. *Cell.* Elsevier;  
908 1993;74: 443–52. doi:10.1016/0092-8674(93)80046-H
- 909 21. Maduro MF, Rothman JH. Making Worm Guts: The Gene Regulatory Network of the  
910 *Caenorhabditis elegans* Endoderm. *Dev Biol.* Academic Press; 2002;246: 68–85.

- 911           doi:10.1006/DBIO.2002.0655
- 912   22.   Maduro MF, Broitman-Maduro G, Mengarelli I, Rothman JH. Maternal deployment of  
913           the embryonic SKN-1 → MED-1,2 cell specification pathway in *C. elegans*. *Dev Biol*.  
914           Academic Press; 2007;301: 590–601. doi:10.1016/J.YDBIO.2006.08.029
- 915   23.   Maduro MF, Meneghini MD, Bowerman B, Broitman-Maduro G, Rothman JH.  
916           Restriction of mesendoderm to a single blastomere by the combined action of SKN-1  
917           and a GSK-3beta homolog is mediated by MED-1 and -2 in *C. elegans*. *Mol Cell*.  
918           2001;7: 475–85. Available: <http://www.ncbi.nlm.nih.gov/pubmed/11463373>
- 919   24.   Maduro MF. Gut development in *C. elegans*. *Semin Cell Dev Biol*. 2017;66: 3–11.  
920           doi:10.1016/j.semcdb.2017.01.001
- 921   25.   Wiesenfahrt T, Osborne Nishimura E, Berg JY, McGhee JD. Probing and rearranging  
922           the transcription factor network controlling the *C. elegans* endoderm. *Worm*. 2016;5:  
923           e1198869. doi:10.1080/21624054.2016.1198869
- 924   26.   Meneghini MD, Ishitani T, Carter JC, Hisamoto N, Ninomiya-Tsuji J, Thorpe CJ, et al.  
925           MAP kinase and Wnt pathways converge to downregulate an HMG-domain repressor  
926           in *Caenorhabditis elegans*. *Nature*. Nature Publishing Group; 1999;399: 793–797.  
927           doi:10.1038/21666
- 928   27.   Shin TH, Yasuda J, Rocheleau CE, Lin R, Soto M, Bei Y, et al. MOM-4, a MAP kinase  
929           kinase kinase-related protein, activates WRM-1/LIT-1 kinase to transduce  
930           anterior/posterior polarity signals in *C. elegans*. *Mol Cell*. 1999;4: 275–80. Available:  
931           <http://www.ncbi.nlm.nih.gov/pubmed/10488343>
- 932   28.   Bei Y, Hogan J, Berkowitz LA, Soto M, Rocheleau CE, Pang KM, et al. SRC-1 and Wnt

- 933 signaling act together to specify endoderm and to control cleavage orientation in  
934 early *C. elegans* embryos. *Dev Cell*. 2002;3: 113–25. Available:  
935 <http://www.ncbi.nlm.nih.gov/pubmed/12110172>
- 936 29. Thorpe CJ, Schlesinger A, Carter JC, Bowerman B. Wnt signaling polarizes an early *C.*  
937 *elegans* blastomere to distinguish endoderm from mesoderm. *Cell*. 1997;90: 695–  
938 705. Available: <http://www.ncbi.nlm.nih.gov/pubmed/9288749>
- 939 30. Nakamura K, Kim S, Ishidate T, Bei Y, Pang K, Shirayama M, et al. Wnt signaling drives  
940 WRM-1/beta-catenin asymmetries in early *C. elegans* embryos. *Genes Dev*. Cold  
941 Spring Harbor Laboratory Press; 2005;19: 1749–54. doi:10.1101/gad.1323705
- 942 31. Rocheleau CE, Yasuda J, Shin TH, Lin R, Sawa H, Okano H, et al. WRM-1 Activates the  
943 LIT-1 Protein Kinase to Transduce Anterior/Posterior Polarity Signals in *C. elegans*.  
944 *Cell*. Cell Press; 1999;97: 717–726. doi:10.1016/S0092-8674(00)80784-9
- 945 32. Owrighi M, Broitman-Maduro G, Luu T, Roberson H, Maduro MF. Roles of the Wnt  
946 effector POP-1/TCF in the *C. elegans* endomesoderm specification gene network. *Dev*  
947 *Biol*. NIH Public Access; 2010;340: 209–21. doi:10.1016/j.ydbio.2009.09.042
- 948 33. Huang S, Shetty P, Robertson SM, Lin R. Binary cell fate specification during *C. elegans*  
949 embryogenesis driven by reiterated reciprocal asymmetry of TCF POP-1 and its  
950 coactivator -catenin SYS-1. *Development*. 2007;134: 2685–2695.  
951 doi:10.1242/dev.008268
- 952 34. Maduro MF, Lin R, Rothman JH. Dynamics of a Developmental Switch: Recursive  
953 Intracellular and Intranuclear Redistribution of *Caenorhabditis elegans* POP-1  
954 Parallels Wnt-Inhibited Transcriptional Repression. *Dev Biol*. Academic Press;



- 955 2002;248: 128–142. doi:10.1006/DBIO.2002.0721
- 956 35. Phillips BT, Kidd AR, King R, Hardin J, Kimble J. Reciprocal asymmetry of SYS-1/beta-  
957 catenin and POP-1/TCF controls asymmetric divisions in *Caenorhabditis elegans*. Proc  
958 Natl Acad Sci. 2007;104: 3231–3236. doi:10.1073/pnas.0611507104
- 959 36. Maduro MF, Kasmir JJ, Zhu J, Rothman JH. The Wnt effector POP-1 and the PAL-  
960 1/Caudal homeoprotein collaborate with SKN-1 to activate *C. elegans* endoderm  
961 development. Dev Biol. 2005;285: 510–523. doi:10.1016/j.ydbio.2005.06.022
- 962 37. Shetty P, Lo M-C, Robertson SM, Lin R. *C. elegans* TCF protein, POP-1, converts from  
963 repressor to activator as a result of Wnt-induced lowering of nuclear levels. Dev Biol.  
964 2005;285: 584–592. doi:10.1016/j.ydbio.2005.07.008
- 965 38. Lin KT-H, Broitman-Maduro G, Hung WWK, Cervantes S, Maduro MF. Knockdown of  
966 SKN-1 and the Wnt effector TCF/POP-1 reveals differences in endomesoderm  
967 specification in *C. briggsae* as compared with *C. elegans*. Dev Biol. 2009;325: 296–  
968 306. doi:10.1016/j.ydbio.2008.10.001
- 969 39. Félix M-A, Braendle C. The natural history of *Caenorhabditis elegans*. Curr Biol.  
970 Elsevier; 2010;20: R965-9. doi:10.1016/j.cub.2010.09.050
- 971 40. Andersen EC, Gerke JP, Shapiro JA, Crissman JR, Ghosh R, Bloom JS, et al.  
972 Chromosome-scale selective sweeps shape *Caenorhabditis elegans* genomic diversity.  
973 Nat Genet. NIH Public Access; 2012;44: 285–90. doi:10.1038/ng.1050
- 974 41. Cook DE, Zdraljevic S, Roberts JP, Andersen EC. CeNDR, the *Caenorhabditis elegans*  
975 natural diversity resource. Nucleic Acids Res. 2017;45: D650–D657.  
976 doi:10.1093/nar/gkw893

- 977 42. Brenner S. The genetics of *Caenorhabditis elegans*. *Genetics*. 1974;77: 71–94.  
978 Available: <http://www.ncbi.nlm.nih.gov/pubmed/4366476>
- 979 43. Kamath RS, Ahringer J. Genome-wide RNAi screening in *Caenorhabditis elegans*.  
980 *Methods*. Academic Press; 2003;30: 313–321. doi:10.1016/S1046-2023(03)00050-1
- 981 44. Rual J-F, Ceron J, Koreth J, Hao T, Nicot A-S, Hirozane-Kishikawa T, et al. Toward  
982 Improving *Caenorhabditis elegans* Phenome Mapping With an ORFeome-Based RNAi  
983 Library. *Genome Res*. 2004;14: 2162–2168. doi:10.1101/gr.2505604
- 984 45. Kamath RS, Fraser AG, Dong Y, Poulin G, Durbin R, Gotta M, et al. Systematic  
985 functional analysis of the *Caenorhabditis elegans* genome using RNAi. *Nature*. Nature  
986 Publishing Group; 2003;421: 231–237. doi:10.1038/nature01278
- 987 46. Sommermann EM, Strohmaier KR, Maduro MF, Rothman JH. Endoderm development  
988 in *Caenorhabditis elegans*: The synergistic action of ELT-2 and -7 mediates the  
989 specification→differentiation transition. *Dev Biol*. 2010;347: 154–166.  
990 doi:10.1016/j.ydbio.2010.08.020
- 991 47. Clokey G V, Jacobson LA. The autofluorescent “lipofuscin granules” in the intestinal  
992 cells of *Caenorhabditis elegans* are secondary lysosomes. *Mech Ageing Dev*. 1986;35:  
993 79–94. Available: <http://www.ncbi.nlm.nih.gov/pubmed/3736133>
- 994 48. Hermann GJ, Schroeder LK, Hieb CA, Kershner AM, Rabbitts BM, Fonarev P, et al.  
995 Genetic Analysis of Lysosomal Trafficking in *Caenorhabditis elegans*. *Mol Biol Cell*.  
996 2005;16: 3273–3288. doi:10.1091/mbc.E05
- 997 49. Kang HM, Zaitlen NA, Wade CM, Kirby A, Heckerman D, Daly MJ, et al. Efficient  
998 Control of Population Structure in Model Organism Association Mapping. *Genetics*.

- 999 2008;178: 1709–1723. doi:10.1534/genetics.107.080101
- 1000 50. Millstein J, Volfson D. Computationally efficient permutation-based confidence  
1001 interval estimation for tail-area FDR. *Front Genet. Frontiers Media SA*; 2013;4: 179.  
1002 doi:10.3389/fgene.2013.00179
- 1003 51. Hansen E, Kerr KF. A Comparison of Two Classes of Methods for Estimating False  
1004 Discovery Rates in Microarray Studies. *Scientifica (Cairo)*. 2012;2012: 1–9.  
1005 doi:10.6064/2012/519394
- 1006 52. Elshire RJ, Glaubitz JC, Sun Q, Poland JA, Kawamoto K, Buckler ES, et al. A Robust,  
1007 Simple Genotyping-by-Sequencing (GBS) Approach for High Diversity Species. Orban  
1008 L, editor. *PLoS One. Public Library of Science*; 2011;6: e19379.  
1009 doi:10.1371/journal.pone.0019379
- 1010 53. Bradbury PJ, Zhang Z, Kroon DE, Casstevens TM, Ramdoss Y, Buckler ES. TASSEL:  
1011 software for association mapping of complex traits in diverse samples.  
1012 *Bioinformatics*. 2007;23: 2633–2635. doi:10.1093/bioinformatics/btm308
- 1013 54. Danecek P, Auton A, Abecasis G, Albers CA, Banks E, DePristo MA, et al. The variant  
1014 call format and VCFtools. *Bioinformatics. Oxford University Press*; 2011;27: 2156–8.  
1015 doi:10.1093/bioinformatics/btr330
- 1016 55. Broman KW, Sen S. *A Guide to QTL Mapping with R/qtl*. New York, NY: Springer New  
1017 York; 2009; 1–20. doi:10.1007/978-0-387-92125-9
- 1018 56. Broman KW, Wu H, Sen S, Churchill GA. R/qtl: QTL mapping in experimental crosses.  
1019 *Bioinformatics*. 2003;19: 889–90. Available:  
1020 <http://www.ncbi.nlm.nih.gov/pubmed/12724300>

- 1021 57. Zhao Z, Boyle TJ, Bao Z, Murray JI, Mericle B, Waterston RH. Comparative analysis of  
1022 embryonic cell lineage between *Caenorhabditis briggsae* and *Caenorhabditis elegans*.  
1023 Dev Biol. NIH Public Access; 2008;314: 93–9. doi:10.1016/j.ydbio.2007.11.015
- 1024 58. Cutter AD. Divergence Times in *Caenorhabditis* and *Drosophila* Inferred from Direct  
1025 Estimates of the Neutral Mutation Rate. Mol Biol Evol. Oxford University Press;  
1026 2008;25: 778–786. doi:10.1093/molbev/msn024
- 1027 59. Sterken MG, Snoek LB, Kammenga JE, Andersen EC. The laboratory domestication of  
1028 *Caenorhabditis elegans*. Trends Genet. NIH Public Access; 2015;31: 224–31.  
1029 doi:10.1016/j.tig.2015.02.009
- 1030 60. Paaby AB, White AG, Riccardi DD, Gunsalus KC, Piano F, Rockman M V. Wild worm  
1031 embryogenesis harbors ubiquitous polygenic modifier variation. Elife. eLife Sciences  
1032 Publications Limited; 2015;4: e09178. doi:10.7554/eLife.09178
- 1033 61. Echeverri CJ, Beachy PA, Baum B, Boutros M, Buchholz F, Chanda SK, et al. Minimizing  
1034 the risk of reporting false positives in large-scale RNAi screens. Nat Methods. 2006;3:  
1035 777–779. doi:10.1038/nmeth1006-777
- 1036 62. Zhuang JJ, Hunter CP. RNA interference in *Caenorhabditis elegans*: Uptake,  
1037 mechanism, and regulation. Parasitology. 2012;139: 560–573.  
1038 doi:10.1017/S0031182011001788
- 1039 63. Raj A, Rifkin SA, Andersen E, van Oudenaarden A. Variability in gene expression  
1040 underlies incomplete penetrance. Nature. Nature Publishing Group; 2010;463: 913–  
1041 918. doi:10.1038/nature08781
- 1042 64. Zhu J, Hill RJ, Heid PJ, Fukuyama M, Sugimoto A, Priess JR, et al. end-1 encodes an

- 1043           apparent GATA factor that specifies the endoderm precursor in *Caenorhabditis*  
1044           *elegans* embryos. *Genes Dev.* Cold Spring Harbor Laboratory Press; 1997;11: 2883–  
1045           96. Available: <http://www.ncbi.nlm.nih.gov/pubmed/9353257>
- 1046   65.   Gleason JE, Korswagen HC, Eisenmann DM. Activation of Wnt signaling bypasses the  
1047           requirement for RTK/Ras signaling during *C. elegans* vulval induction. *Genes Dev.* Cold  
1048           Spring Harbor Laboratory Press; 2002;16: 1281–90. doi:10.1101/gad.981602
- 1049   66.   Wang J, Zaitlen NA, Wade CM, Kirby A, Heckerman D, Daly MJ, et al. An estimator for  
1050           pairwise relatedness using molecular markers. *Genetics.* *Genetics*; 2002;160: 1203–  
1051           15. doi:10.1534/genetics.167.1.531
- 1052   67.   Rieseberg LH, Widmer A, Arntz AM, Burke B. The genetic architecture necessary for  
1053           transgressive segregation is common in both natural and domesticated populations.  
1054           *Philos Trans R Soc B Biol Sci.* 2003;358: 1141–1147. doi:10.1098/rstb.2003.1283
- 1055   68.   Ruf V, Holzem C, Peyman T, Walz G, Blackwell TK, Neumann-Haefelin E. TORC2  
1056           signaling antagonizes SKN-1 to induce *C. elegans* mesendodermal embryonic  
1057           development. *Dev Biol.* Academic Press; 2013;384: 214–227.  
1058           doi:10.1016/J.YDBIO.2013.08.011
- 1059   69.   Witze ES, Field ED, Hunt DF, Rothman JH. *C. elegans* pur alpha, an activator of end-1,  
1060           synergizes with the Wnt pathway to specify endoderm. *Dev Biol.* 2009;327: 12–23.  
1061           doi:10.1016/j.ydbio.2008.11.015
- 1062   70.   Walston T, Tuskey C, Edgar L, Hawkins N, Ellis G, Bowerman B, et al. Multiple Wnt  
1063           Signaling Pathways Converge to Orient the Mitotic Spindle in Early *C. elegans*  
1064           Embryos. *Dev Cell.* Cell Press; 2004;7: 831–841. doi:10.1016/J.DEVCEL.2004.10.008

- 1065 71. Tatebe H, Shiozaki K. Evolutionary Conservation of the Components in the TOR  
1066 Signaling Pathways. *Biomolecules*. 2017;7: 77. doi:10.3390/biom7040077
- 1067 72. Adoutte A, Philippe H. The major lines of metazoan evolution: summary of traditional  
1068 evidence and lessons from ribosomal RNA sequence analysis. *EXS*. 1993;63: 1–30.  
1069 Available: <http://www.ncbi.nlm.nih.gov/pubmed/8422536>
- 1070 73. Kalinka AT, Varga KM, Gerrard DT, Preibisch S, Corcoran DL, Jarrells J, et al. Gene  
1071 expression divergence recapitulates the developmental hourglass model. *Nature*.  
1072 Nature Publishing Group; 2010;468: 811–814. doi:10.1038/nature09634
- 1073 74. Raff RA. *The shape of life : genes, development, and the evolution of animal form*.  
1074 University of Chicago Press; 1996.
- 1075 75. Domazet-Lošo T, Tautz D. A phylogenetically based transcriptome age index mirrors  
1076 ontogenetic divergence patterns. *Nature*. Nature Publishing Group; 2010;468: 815–  
1077 818. doi:10.1038/nature09632
- 1078 76. Coroian C, Broitman-Maduro G, Maduro MF. Med-type GATA factors and the  
1079 evolution of mesendoderm specification in nematodes. *Dev Biol*. 2006;289: 444–455.  
1080 doi:10.1016/j.ydbio.2005.10.024
- 1081 77. Maduro MF, Hill RJ, Heid PJ, Newman-Smith ED, Zhu J, Priess JR, et al. Genetic  
1082 redundancy in endoderm specification within the genus *Caenorhabditis*. *Dev Biol*.  
1083 2005;284: 509–522. doi:10.1016/j.ydbio.2005.05.016
- 1084 78. Mensch J, Serra F, Lavagnino NJ, Dopazo H, Hasson E. Positive Selection in  
1085 Nucleoporins Challenges Constraints on Early Expressed Genes in *Drosophila*  
1086 Development. *Genome Biol Evol*. 2013;5: 2231–2241. doi:10.1093/gbe/evt156

- 1087 79. Davis GK, Patel NH. Short, Long, and Beyond: Molecular and Embryological  
1088 Approaches to Insect Segmentation. *Annu Rev Entomol. Annual Reviews* 4139 El  
1089 Camino Way, P.O. Box 10139, Palo Alto, CA 94303-0139, USA ; 2002;47: 669–699.  
1090 doi:10.1146/annurev.ento.47.091201.145251
- 1091 80. Lynch JA, El-Sherif E, Brown SJ. Comparisons of the embryonic development of  
1092 *Drosophila*, *Nasonia*, and *Tribolium*. *Wiley Interdiscip Rev Dev Biol.* John Wiley &  
1093 Sons, Ltd (10.1111); 2012;1: 16–39. doi:10.1002/wdev.3
- 1094 81. Atallah J, Lott SE. Evolution of maternal and zygotic mRNA complements in the early  
1095 *Drosophila* embryo. Dyer KA, editor. *PLOS Genet.* 2018;14: e1007838.  
1096 doi:10.1371/journal.pgen.1007838
- 1097 82. Vu V, Verster AJ, Schertzberg M, Chuluunbaatar T, Spensley M, Pajkic D, et al. Natural  
1098 Variation in Gene Expression Modulates the Severity of Mutant Phenotypes. *Cell.*  
1099 2015;162: 391–402. doi:10.1016/j.cell.2015.06.037
- 1100 83. Moore JH, Williams SM. Epistasis and Its Implications for Personal Genetics. *Am J*  
1101 *Hum Genet.* Cell Press; 2009;85: 309–320. doi:10.1016/J.AJHG.2009.08.006
- 1102 84. Page GP, George V, Go RC, Page PZ, Allison DB. “Are We There Yet?”: Deciding When  
1103 One Has Demonstrated Specific Genetic Causation in Complex Diseases and  
1104 Quantitative Traits. *Am J Hum Genet.* 2003;73: 711–719. doi:10.1086/378900
- 1105 85. Mackay TFC. Epistasis and quantitative traits: using model organisms to study gene-  
1106 gene interactions. *Nat Rev Genet.* NIH Public Access; 2014;15: 22–33.  
1107 doi:10.1038/nrg3627
- 1108 86. Volis S, Shulgina I, Zaretsky M, Koren O. Epistasis in natural populations of a

- 1109           predominantly selfing plant. *Heredity* (Edinb). Nature Publishing Group; 2011;106:  
1110           300–9. doi:10.1038/hdy.2010.79
- 1111   87.   Félix M-A. Cryptic Quantitative Evolution of the Vulva Intercellular Signaling Network  
1112           in *Caenorhabditis*. *Curr Biol*. 2007;17: 103–114. doi:10.1016/j.cub.2006.12.024
- 1113   88.   Barkoulas M, van Zon JS, Milloz J, van Oudenaarden A, Félix M-A. Robustness and  
1114           Epistasis in the *C. elegans* Vulval Signaling Network Revealed by Pathway Dosage  
1115           Modulation. *Dev Cell*. Cell Press; 2013;24: 64–75. doi:10.1016/J.DEVCEL.2012.12.001
- 1116   89.   Duveau F, Félix M-A. Role of Pleiotropy in the Evolution of a Cryptic Developmental  
1117           Variation in *Caenorhabditis elegans*. Noor MAF, editor. *PLoS Biol*. Public Library of  
1118           Science; 2012;10: e1001230. doi:10.1371/journal.pbio.1001230
- 1119   90.   Johnson NA, Porter AH. Evolution of branched regulatory genetic pathways:  
1120           directional selection on pleiotropic loci accelerates developmental system drift.  
1121           *Genetica*. Springer Netherlands; 2006;129: 57–70. doi:10.1007/s10709-006-0033-2
- 1122   91.   Phillips PC. Epistasis--the essential role of gene interactions in the structure and  
1123           evolution of genetic systems. *Nat Rev Genet*. NIH Public Access; 2008;9: 855–67.  
1124           doi:10.1038/nrg2452
- 1125   92.   Wagner GP, Zhang J. The pleiotropic structure of the genotype–phenotype map: the  
1126           evolvability of complex organisms. *Nat Rev Genet*. Nature Publishing Group; 2011;12:  
1127           204–213. doi:10.1038/nrg2949
- 1128   93.   Shafer B, Onishi K, Lo C, Colakoglu G, Zou Y. Vangl2 Promotes Wnt/Planar Cell  
1129           Polarity-like Signaling by Antagonizing Dvl1-Mediated Feedback Inhibition in Growth  
1130           Cone Guidance. *Dev Cell*. Cell Press; 2011;20: 177–191.



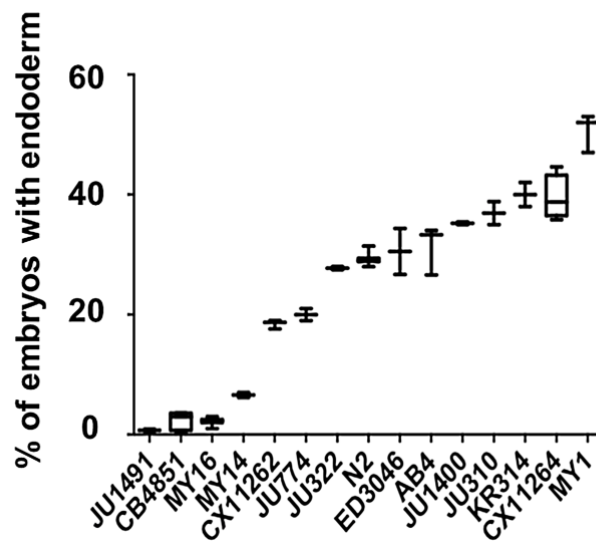
- 1131           doi:10.1016/J.DEVCEL.2011.01.002
- 1132   94.   Zheng C, Diaz-Cuadros M, Chalfie M. Dishevelled attenuates the repelling activity of  
1133           Wnt signaling during neurite outgrowth in *Caenorhabditis elegans*. Proc Natl Acad Sci  
1134           U S A. National Academy of Sciences; 2015;112: 13243–8.  
1135           doi:10.1073/pnas.1518686112
- 1136   95.   Rivera-Pomar R, Jäckle H. From gradients to stripes in *Drosophila* embryogenesis:  
1137           filling in the gaps. Trends Genet. Elsevier Current Trends; 1996;12: 478–483.  
1138           doi:10.1016/0168-9525(96)10044-5
- 1139   96.   Maduro MF, Broitman-Maduro G, Choi H, Carranza F, Wu AC-Y, Rifkin SA. MED GATA  
1140           factors promote robust development of the *C. elegans* endoderm. Dev Biol. Academic  
1141           Press; 2015;404: 66–79. doi:10.1016/J.YDBIO.2015.04.025
- 1142   97.   Choi H, Broitman-Maduro G, Maduro MF. Partially compromised specification causes  
1143           stochastic effects on gut development in *C. elegans*. Dev Biol. Academic Press;  
1144           2017;427: 49–60. doi:10.1016/J.YDBIO.2017.05.007
- 1145   98.   Maduro MF. Developmental robustness in the *Caenorhabditis elegans* embryo. Mol  
1146           Reprod Dev. 2015;82: 918–931. doi:10.1002/mrd.22582
- 1147   99.   Zhan T, Rindtorff N, Boutros M. Wnt signaling in cancer. Oncogene. Nature Publishing  
1148           Group; 2017;36: 1461–1473. doi:10.1038/onc.2016.304
- 1149   100.   Jenkins ZA, van Kogelenberg M, Morgan T, Jeffs A, Fukuzawa R, Pearl E, et al.  
1150           Germline mutations in WTX cause a sclerosing skeletal dysplasia but do not  
1151           predispose to tumorigenesis. Nat Genet. 2009;41: 95–100. doi:10.1038/ng.270
- 1152   101.   Baron R, Gori F. Targeting WNT signaling in the treatment of osteoporosis. Curr Opin

- 1153 Pharmacol. Elsevier; 2018;40: 134–141. doi:10.1016/J.COPH.2018.04.011
- 1154 102. Chen N, Wang J. Wnt/ $\beta$ -Catenin Signaling and Obesity. *Front Physiol.* 2018;9: 792.  
1155 doi:10.3389/fphys.2018.00792
- 1156 103. Schinner S. Wnt-signalling and the Metabolic Syndrome. *Horm Metab Res.* 2009;41:  
1157 159–163. doi:10.1055/s-0028-1119408
- 1158 104. Gibson G, Dworkin I. Uncovering cryptic genetic variation. *Nat Rev Genet. Nature*  
1159 *Publishing Group*; 2004;5: 681–690. doi:10.1038/nrg1426
- 1160 105. Frankel N, Davis GK, Vargas D, Wang S, Payre F, Stern DL. Phenotypic robustness  
1161 conferred by apparently redundant transcriptional enhancers. *Nature.* 2010;466:  
1162 490–493. doi:10.1038/nature09158
- 1163 106. Mohun T. Muscle differentiation. *Curr Opin Cell Biol.* 1992;4: 923–8. Available:  
1164 <http://www.ncbi.nlm.nih.gov/pubmed/1485959>
- 1165 107. Imai Y, Gates MA, Melby AE, Kimelman D, Schier AF, Talbot WS. The homeobox genes  
1166 *vox* and *vent* are redundant repressors of dorsal fates in zebrafish. *Development.*  
1167 2001;128: 2407–20. Available: <http://www.ncbi.nlm.nih.gov/pubmed/11493559>
- 1168 108. Manley NR, Capecchi MR. Hox Group 3 Paralogous Genes Act Synergistically in the  
1169 Formation of Somitic and Neural Crest-Derived Structures. *Dev Biol. Academic Press*;  
1170 1997;192: 274–288. doi:10.1006/DBIO.1997.8765
- 1171 109. Nam J, Nei M. Evolutionary change of the numbers of homeobox genes in bilateral  
1172 animals. *Mol Biol Evol. NIH Public Access*; 2005;22: 2386–94.  
1173 doi:10.1093/molbev/msi229

- 1174 110. Yoon CH, Chang C, Hopper NA, Lesa GM, Sternberg PW. Requirements of multiple  
1175 domains of SLI-1, a *Caenorhabditis elegans* homologue of c-Cbl, and an inhibitory  
1176 tyrosine in LET-23 in regulating vulval differentiation. *Mol Biol Cell*. American Society  
1177 for Cell Biology; 2000;11: 4019–31. Available:  
1178 <http://www.ncbi.nlm.nih.gov/pubmed/11071924>
- 1179 111. Braendle C, Félix M-A. Plasticity and Errors of a Robust Developmental System in  
1180 Different Environments. *Dev Cell*. 2008;15: 714–724.  
1181 [doi:10.1016/j.devcel.2008.09.011](https://doi.org/10.1016/j.devcel.2008.09.011)
- 1182 112. Grimbert S, Vargas Velazquez AM, Braendle C. Physiological Starvation Promotes  
1183 *Caenorhabditis elegans* Vulval Induction. *G3 (Bethesda)*. Genetics Society of America;  
1184 2018;8: 3069–3081. [doi:10.1534/g3.118.200449](https://doi.org/10.1534/g3.118.200449)
- 1185 113. Zheng M, Messerschmidt D, Jungblut B, Sommer RJ. Conservation and diversification  
1186 of Wnt signaling function during the evolution of nematode vulva development. *Nat*  
1187 *Genet*. 2005;37: 300–304. [doi:10.1038/ng1512](https://doi.org/10.1038/ng1512)
- 1188 114. Wang X, Sommer RJ. Antagonism of LIN-17/*Frizzled* and LIN-18/*Ryk* in Nematode  
1189 Vulva Induction Reveals Evolutionary Alterations in Core Developmental Pathways.  
1190 Sternberg PW, editor. *PLoS Biol*. 2011;9: e1001110.  
1191 [doi:10.1371/journal.pbio.1001110](https://doi.org/10.1371/journal.pbio.1001110)
- 1192 115. Zalts H, Yanai I. Developmental constraints shape the evolution of the nematode mid-  
1193 developmental transition. *Nat Ecol Evol*. Nature Publishing Group; 2017;1: 0113.  
1194 [doi:10.1038/s41559-017-0113](https://doi.org/10.1038/s41559-017-0113)

1195

1196 **Supplementary figures**

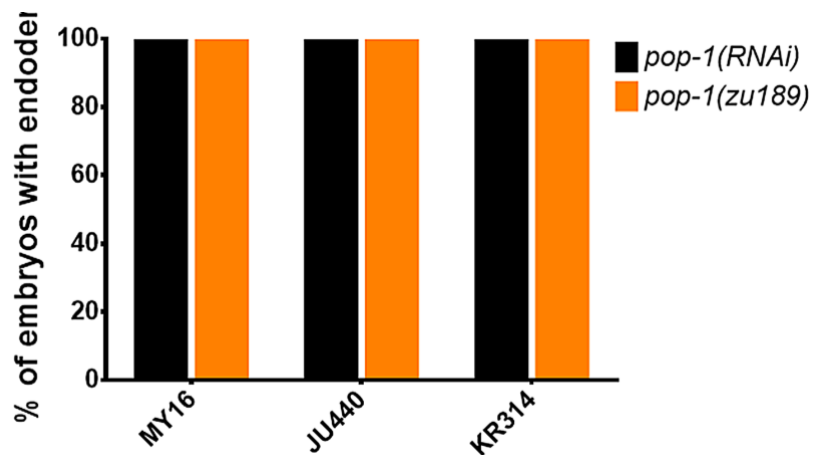


1197

1198 **Supplementary Fig. 1: High reproducibility of *skn-1*(RNAi) phenotypes in various *C. elegans* isotypes.**

1199 *A minimum of two replicates were obtained, with >500 embryos per replicate. Box-plot represents median*  
1200 *with range bars showing upper and lower quartiles.*

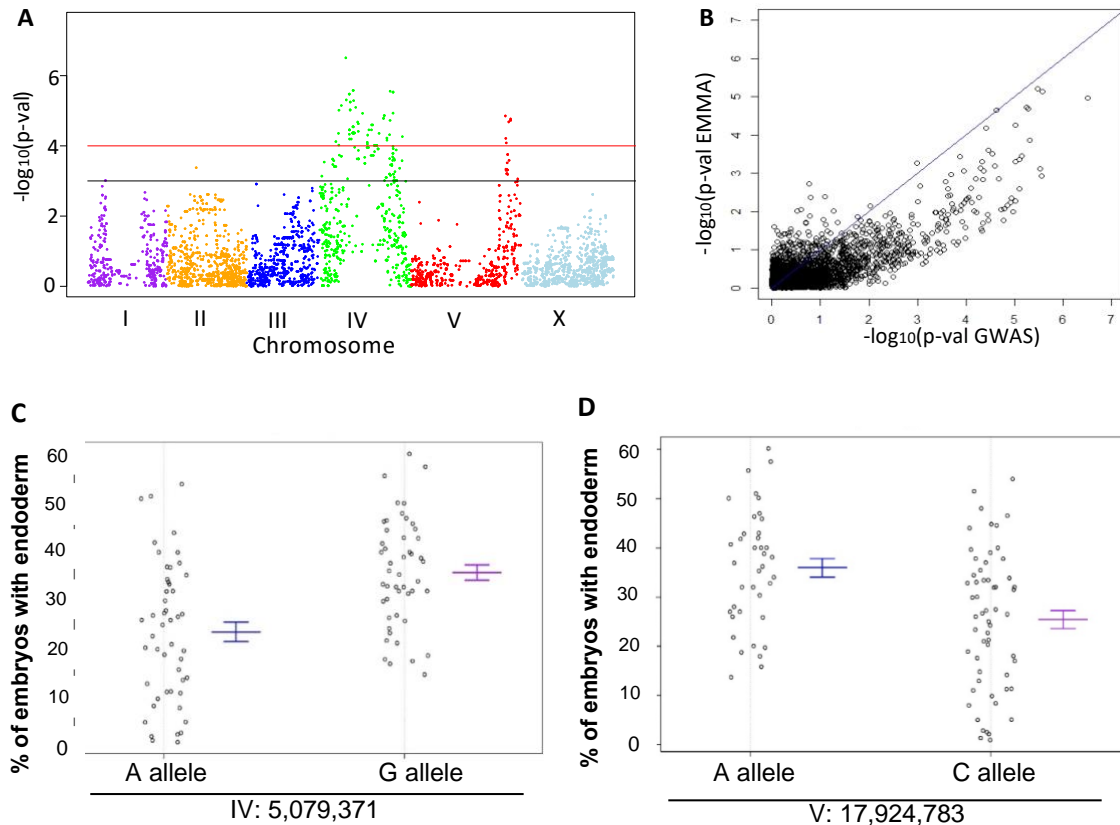
1201



1202

1203 **Supplementary Fig. 2: The requirement for POP-1 in endoderm formation does not vary in three**  
1204 **introgressed strains.**

1205 *Strains are shown on the x-axis and fraction of arrested embryos with endoderm are shown on the y-axis.*  
1206 *Four introgressed lines were studied for each mutant strain. >200 embryos were scored per experiment.*

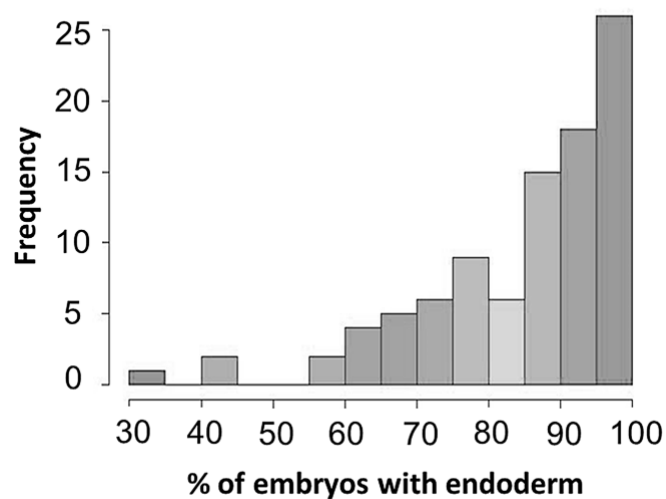


1207

1208 **Supplementary Fig. 3: linear model GWAS of *skn-1* embryonic phenotype highly correlates with the**  
1209 **mixed-model analysis.**

1210 (A) Manhattan plot of *skn-1*(RNAi) GWAS. Red line represents 1.5% FDR (obtained from 10,000 permuted  
1211 results) and black line represents 3.0% FDR. The chromosomes are color-coded. The y axis is the  $-\log_{10}$  of p-  
1212 value. (B) Correlation between *skn-1*(RNAi) GWAS and EMMA (see Fig. 5A). y-axis is the  $-\log_{10}$  of the p-  
1213 values from EMMA, x-axis is  $-\log_{10}$  of the p-values from GWAS. A modest linear relationship is found  
1214 (Spearman correlation coefficient = 0.43) as shown by the blue line. (C) Effect plot of the top SNP revealed  
1215 by *skn-1*(RNAi) EMMA (see Fig. 5A). (D) Effect plot of the top SNP on Chromosome V revealed by *skn-1*(RNAi)  
1216 GWAS. The variant position and genotype are shown on the x-axis, while the phenotype of strains carrying  
1217 the alleles after *skn-1*(RNAi) treatment is shown on the y-axis. Confidence intervals for the average  
1218 phenotype in each genotype group are shown.

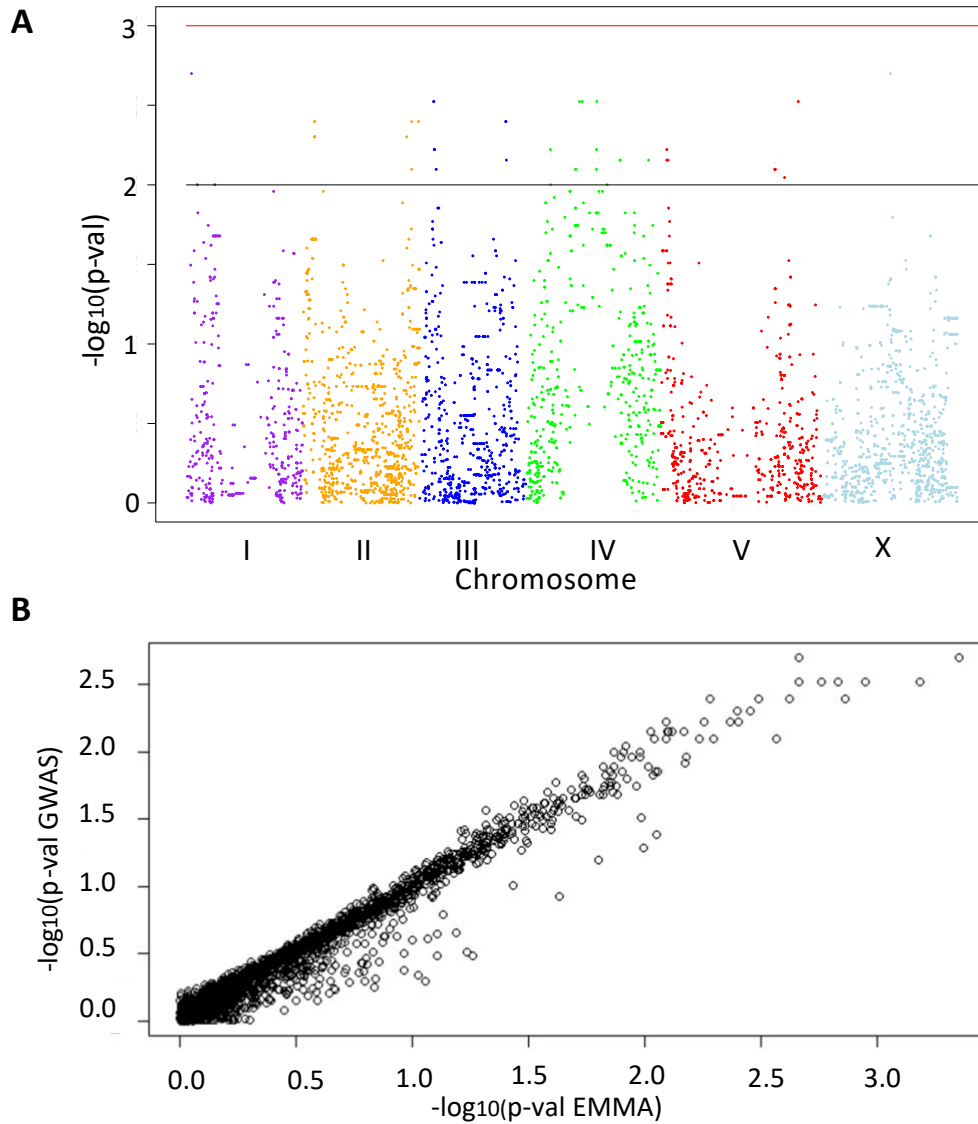
1219



1220

1221 **Supplementary Fig. 4: Histogram of *mom-2*(RNAi) phenotype among the 94 wild isolates.**

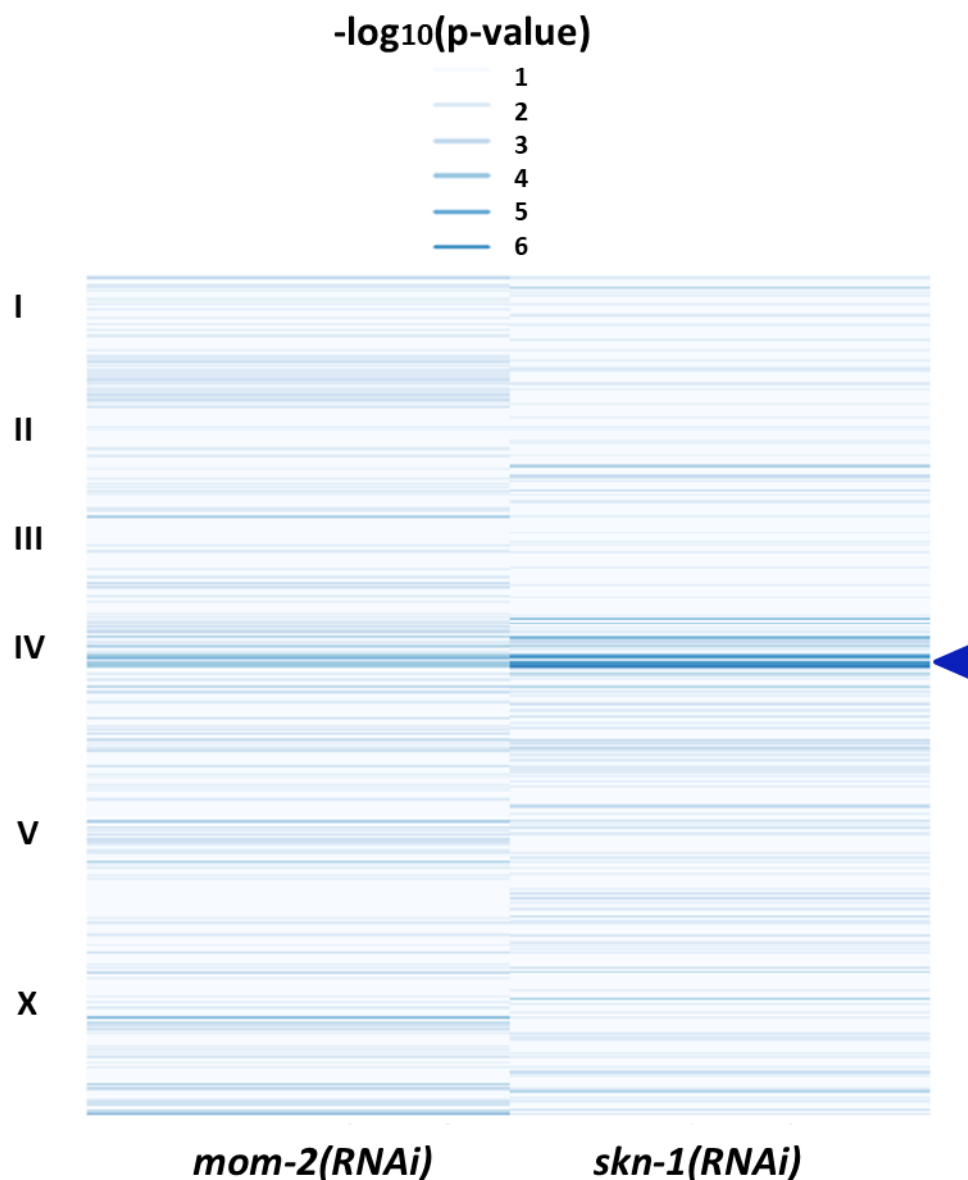
1222 A beta-distribution is observed (skewed to the right). Shapiro-Wilk normality test ( $W=0.8682$ ,  $p$ -  
1223 value= $1.207 \times 10^{-7}$ ).



1224

1225 **Supplementary Fig. 5: GWAS of *mom-2* embryonic phenotype is highly correlated with the mixed-**  
1226 **model analysis.**

1227 (A) Manhattan plot of *mom-2(RNAi)* GWAS (permutation-adjusted p-values). Black line represents p-  
1228 value<0.01, while red line represents p-value<0.001. Genomic regions are shown on the x-axis. The  
1229 chromosomes are color-coded. The y axis is the  $-\log_{10}$  of p-value in the linear model. (B) Correlation  
1230 between *mom-2(RNAi)* GWAS and EMMA. The y-axis represents the  $-\log_{10}$  of the p-values from the GWAS  
1231 approach, while the x-axis represents  $-\log_{10}$  of the p-values from the EMMA approach. A strong linear  
1232 relationship is found (Pearson's correlation  $R = 0.95$ , p-value <  $2.2e-16$ ).

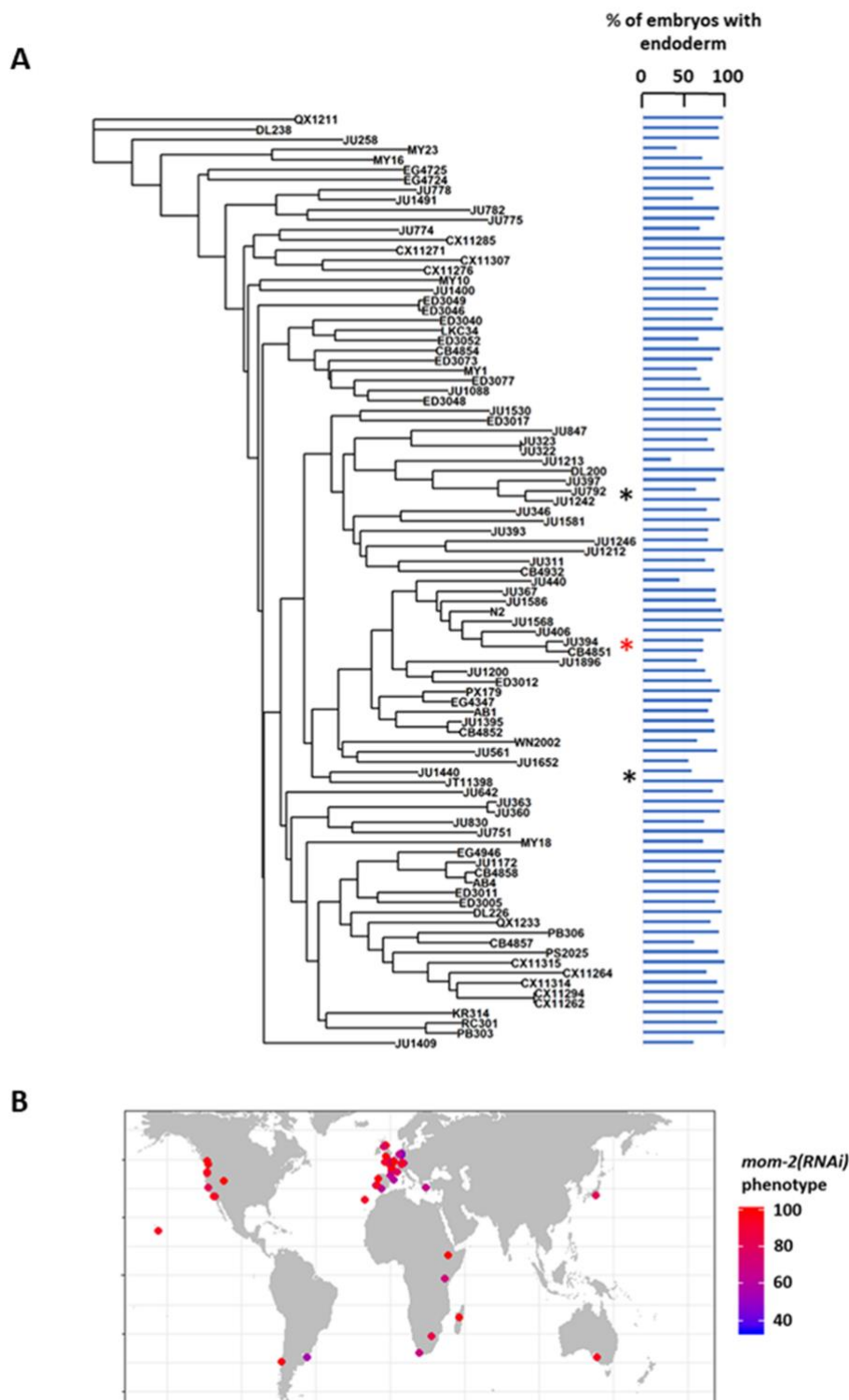


1233

1234 **Supplementary Fig. 6: Comparison of EMMA p-values for both *mom-2* and *skn-1* RNAi phenotypes.**

1235 Heatmap of p-values for *mom-2*(RNAi) (left) and *skn-1*(RNAi) (right) as calculated in the EMMA analyses  
1236 (see Fig. 5A, B). Strength of association between genotype and endoderm formation phenotypes is  
1237 represented as  $-\log_{10}(p\text{-value})$ , here depicted as a heatmap (lighter colors – weaker association, darker  
1238 colors – stronger association). An overlap (indicated by arrow head) is found in a small region of  
1239 chromosome IV, but no further correlations are observed.

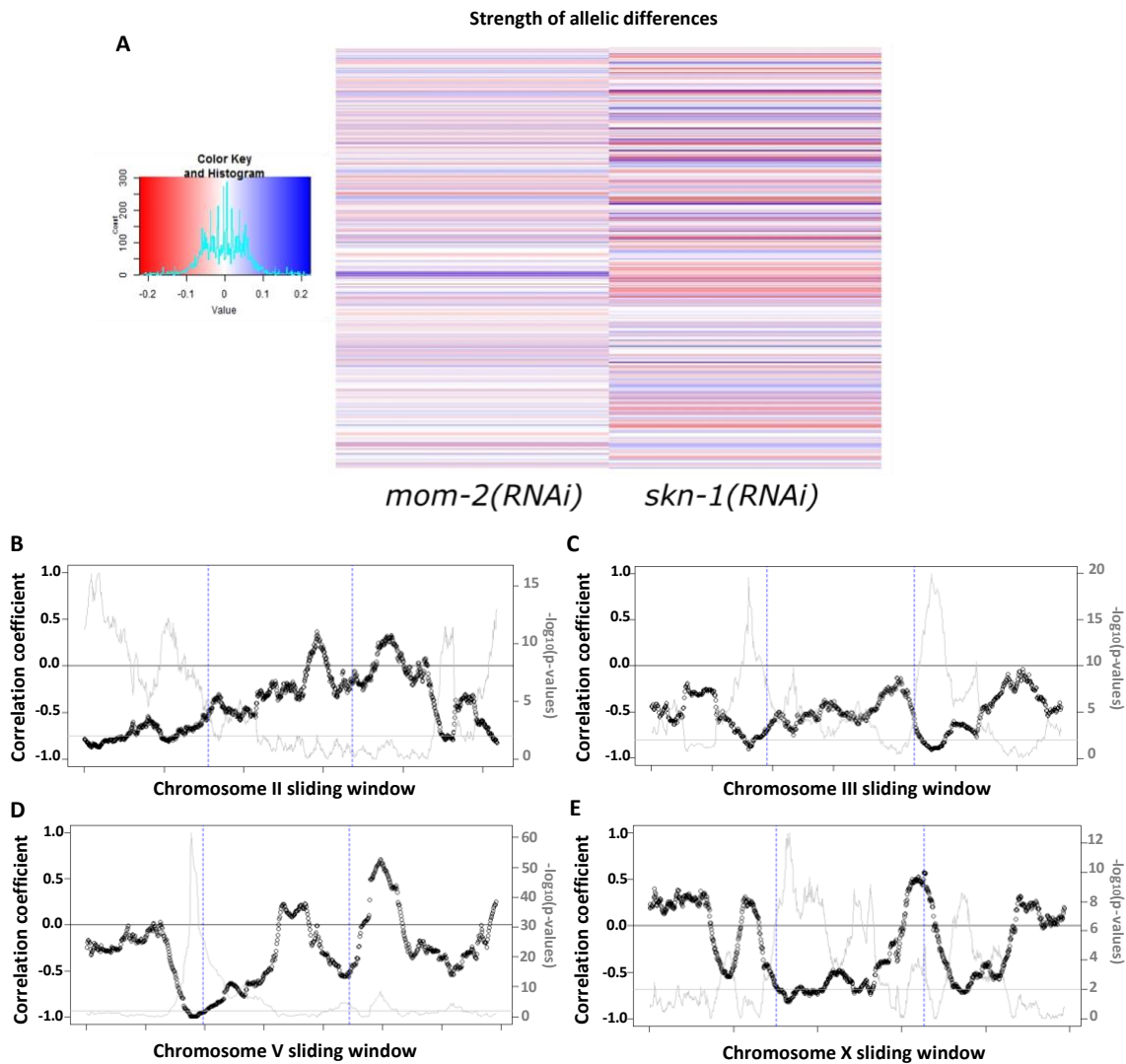




1240

1241 **Supplementary Fig. 7: MOM-2 requirement does not correlate with genotypic relatedness or**  
 1242 **geographical location.**

1243 (A) *mom-2* (RNAi) phenotype of 94 isolates arranged with respect to the neighbor-joining tree constructed  
 1244 using 4,690 SNPs and pseudo-rooted to QX1211. Red asterisk indicates an example of closely related strains  
 1245 (JU394 and CB4851) with similar phenotypes, while black asterisks indicate examples sister strains (JU792  
 1246 and JU1242; JU1440 and JT11398) with distinct phenotypes. (B) Worldwide distribution of *mom-2*(RNAi)  
 1247 phenotype across 94 isolates. Each circle represents a single isolate.



1248

1249 **Supplementary Fig. 8: Negative correlation of *skn-1(RNAi)* and *mom-2(RNAi)* allelic differences.**

1250 (A) Heat map of allelic differences per SNP for *skn-1(RNAi)* and *mom-2(RNAi)*, as calculated by the  
 1251 phenotypic median differences per allele at each SNP. Each line represents a color-coded result of a single  
 1252 locus, covering the entire genome. Correlation sliding window of (B) chromosome II, (C) chromosome III, (D)  
 1253 chromosome V and (E) chromosome X. Windows of 50 SNPs were used to calculate the correlation  
 1254 coefficient and p-value. Black circles represent the correlation coefficient (R value) for each window (scale  
 1255 on the x-axis). Black line indicates the 0 threshold. Grey line represents the  $-\log_{10}$  of the p-values for the  
 1256 corresponding correlation windows (scale on the y-axis). Grey horizontal line is the significance threshold  
 1257 set at  $p$ -value=0.01. Dotted blue lines divide chromosomal region into left, middle and right arms.